ROBOMECH Journal

RESEARCH ARTICLE

Open Access

# Suction pad unit using a bellows pneumatic actuator as a support mechanism for an end effector of depalletizing robots

Junya Tanaka*, Akihito Ogawa, Hideichi Nakamoto, Takafumi Sonoura and Haruna Eto

**Abstract**

This paper describes a vacuum suction-type end effector for depalletizing robots in distribution centers. The developed end effector has multiple suction pad units to which a bellows pneumatic actuator is applied as the support mechanism. Load-bearing capacity is improved due to a high-strength wire provided inside the bellows, and the contraction force is improved due to ring members placed inside of the ridges of the rubber bellows. The developed end effector is attached to the arm of a linear motion-type depalletizing robot, and its real-world performance is verified. Verification results confirm that the suction pad units tolerate cardboard box inclination and differences in box height by a simple lowering motion of the arm, and multiple cardboard boxes can be simultaneously unloaded. Moreover, as compared with conventional end effectors, the developed end effector achieves large expansion and contraction in a thin structure. The developed end effector is expected to broaden applications for depalletizing robots.

**Keywords:** Depalletizing robot, Logistics site, Transfer method, Hardware design, Pneumatic actuator

## Background

The recent spread of e-commerce has increased logistics distribution volumes. However, securing additional workers at logistics sites in Japan has become difficult due to an aging population and declining workforce. Logistics companies are therefore actively automating their distribution facilities. Potential tasks for automation include sequential unloading of cardboard boxes from a roll box pallet and loading onto a conveyor (Fig. 1). Long hours of unloading work places a heavy physical burden on workers, leading to work-related injuries such as back problems. As Fig. 2 shows, a roll box pallet is a carriage on casters with three fenced faces on the outer periphery and one open side. Models include those with and without a middle shelf (Fig. 2a, b, respectively).

Depalletizing robots using industrial robot arms [1–3] have been proposed, but outstanding problems include large installation spaces and the complex motion trajectory needed to avoid contact between the roll box pallet and the robot arm. Therefore, we developed the linear motion-type depalletizing robot shown in Figs. 3 and 4 for system compactification and motion trajectory simplification [4]. The developed robot consists of a main arm with an end effector for unloading boxes and a conveyor arm with a belt conveyor for carrying unloaded boxes. Fifty conventional suction pad units (VPC 50-50 BN 6 JC, PISCO), shown in Fig. 5, were used for the conventional end effector. The suction pad unit is mainly composed of a suction pad, a support mechanism, and a connecting part. In the suction pad, internal pressure in the space between the suction pad and cardboard box is lowered below atmospheric pressure by a pressure-reducing device such as a vacuum pump, and the cardboard box is held by that pressure difference. These suction pads can hold various objects, and so are also applied to many other logistics robots [5–9]. Existing suction gripper designs can be broadly categorized as configurations with only suction pads [6, 9] and those with suction pads and multi-fingered

*Correspondence: junya1.tanaka@toshiba.co.jp
Corporate Research & Development Center, Toshiba Corporation, 1, Komukai Toshiba-cho, Saiwai-ku, Kawasaki-shi, Kanagawa 212-8582, Japan


**Fig. 1** Unloading operation

hands [5, 7, 8]. Focusing on only suction pad operations, these can be divided into structures in which suction pad support members are bent [6–8] and those in which they are bent and expanded [5, 9]. When suction pad support members are bent and expanded, suction pads can hold objects in various orientations.

In commercially available suction pad units, the distance between the connecting part and the suction pad is kept constant by springs arranged along the support mechanism. When the suction pad contacts the cardboard box, a shaft member in the support mechanism protrudes from the connecting part due to reduced distance between the connecting part and the suction pad. To improve processing capacity in unloading operations, the end effector can simultaneously hold multiple cardboard boxes by suction in one unloading operation. Height differences between boxes are compensated for by expansion or contraction of the support mechanism for the suction pad unit.

Various verification experiments have revealed the following problems in conventional end effectors that simply combine commercially available suction pad units.

- When the suction pad contacts the upper surface of a cardboard box, the box may be crushed by the pressing force of a spring along the support mechanism. In conventional suction pad units, the ability to follow surfaces depends on the suction pad's material and shape, and pressing suction pads against an inclined surface can crush boxes.
- Considering future developments toward linear motion-type depalletizing robots, end effectors must be sufficiently thin to enter the narrow gap directly beneath the middle shelf of a roll box pallet. However, the structures of commercially available suction

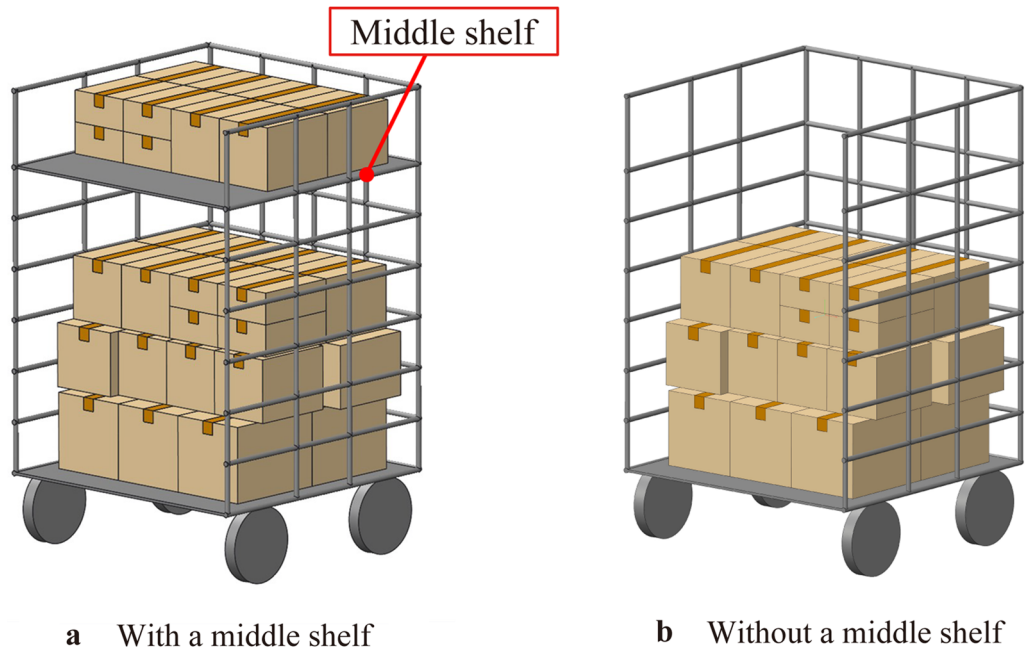


**Fig. 2** A roll box pallet. **a** With a middle shelf, **b** without a middle shelf

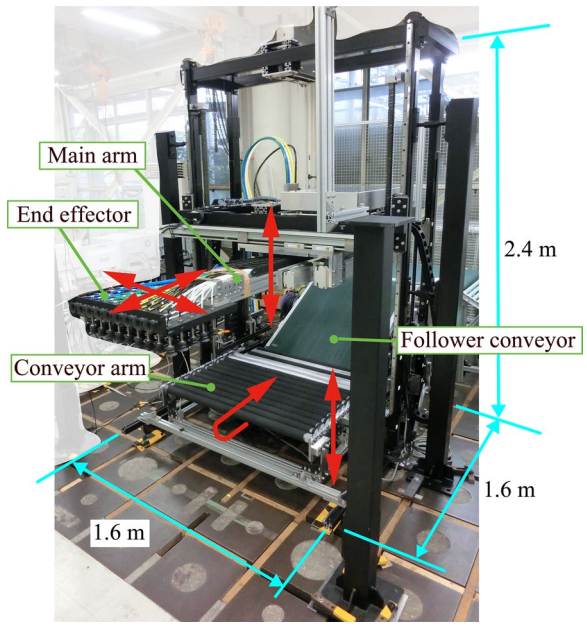


**Fig. 3** Developed linear motion-type depalletizing robot [4]

pad units make it is difficult to achieve large expansion and contraction while also reducing size.

We therefore aimed at realizing a small pressing force with high ability to follow inclined surfaces by devising a support mechanism for suction pad units that realizes both reduced size and large amounts of expansion and contraction. Expansion and contraction operations by the support mechanism are actively driven to accommodate various cardboard box states. To reduce cost by unifying drive sources, the support mechanism is pneumatically driven, as with the suction pads. Various pneumatic actuators have been proposed [10–24]. McKibben-type artificial muscles [10–14] have the characteristic of expanding diametrically and contracting in the axial direction when pressurized. Flat tubes [15, 16] deform in the diametrical direction when pressurized. There are also structures that bend by pressurizing their internal space [17–20]. However, pneumatic actuators that are deformed by pressure risk expansion damage unless proper control is performed. In contrast, bellows-type actuators [21–24] contract in the axial direction when decompressed and extend in the axial direction after releasing the reduced pressure state, so pressurization beyond atmospheric pressure is unnecessary. Therefore, from the viewpoint of safety, we adopted the bellows method for the pneumatic actuator used in this study. However, a conventional bellows pneumatic actuator is required to increase load-bearing capacity and contraction force while maintaining flexibility in a simple configuration.

In this study, we developed an end effector with multiple suction pad units using a bellows pneumatic actuator as the support mechanism and verified the mechanism from the viewpoint of expanding applications for linear motion-type depalletizing robots. Load resistance was improved by providing a strong wire inside the bellows, and contraction force was improved by inserting ring members inside the ridges of the bellows. The developed end effector was attached to the main arm of a conventional linear motion-type depalletizing robot, and its real-world performance was verified. Here, we report the design principles, actual mechanism, and system configuration, and experimental results regarding holding operations of the developed suction pad unit and end effector.

## Methods

### Terminology

Main terms in this paper are "expansion and contraction", "load-bearing capacity," and "contraction force." The "expansion and contraction" of a suction pad refers to displacement of its support mechanism. "Load-bearing capacity" refers to ability to maintain the stretched state without damaging the bellows pneumatic actuator. "Contraction force" is force generated by reducing pressure in the bellows pneumatic actuator.

### Cardboard box for unloading

Cardboard boxes of various sizes are handled in logistics facilities, but boxes may be of a predetermined single size in a logistics warehouse used for a specific retailer. We thus assumed a logistics warehouse with four types of cardboard boxes, shown in Fig. 6 and Table 1. Although the mass of a cardboard box is often as much as 5 kg, the maximum target weight was set to 30 kg, which is the upper limit for a parcel delivery service. The assumed loading condition was cardboard boxes of varied sizes on a roll box pallet.

We investigated height differences between the four cardboard box types, which vary according to the load state. Table 2 shows the height difference of each box when one of each of the four box types is placed on the bottom of the roll box pallet. The lower limit on height differences between the target cardboard boxes was set to 40 mm, and the upper limit was set to twice that, 80 mm.

Regarding box inclination, we assumed that boxes move due to vibration during roll box pallet transport, causing inclination due to height differences. Assuming an upper limit of 80 mm on height differences, box ① is most inclined along its shortest edge (W: 280 mm) due to the height difference at a position 80 mm above the horizontal plane. Since the inclination of box ① was about 16.7° from the geometrical relation, the assumed maximum inclination for a cardboard box was set to 20.0°.

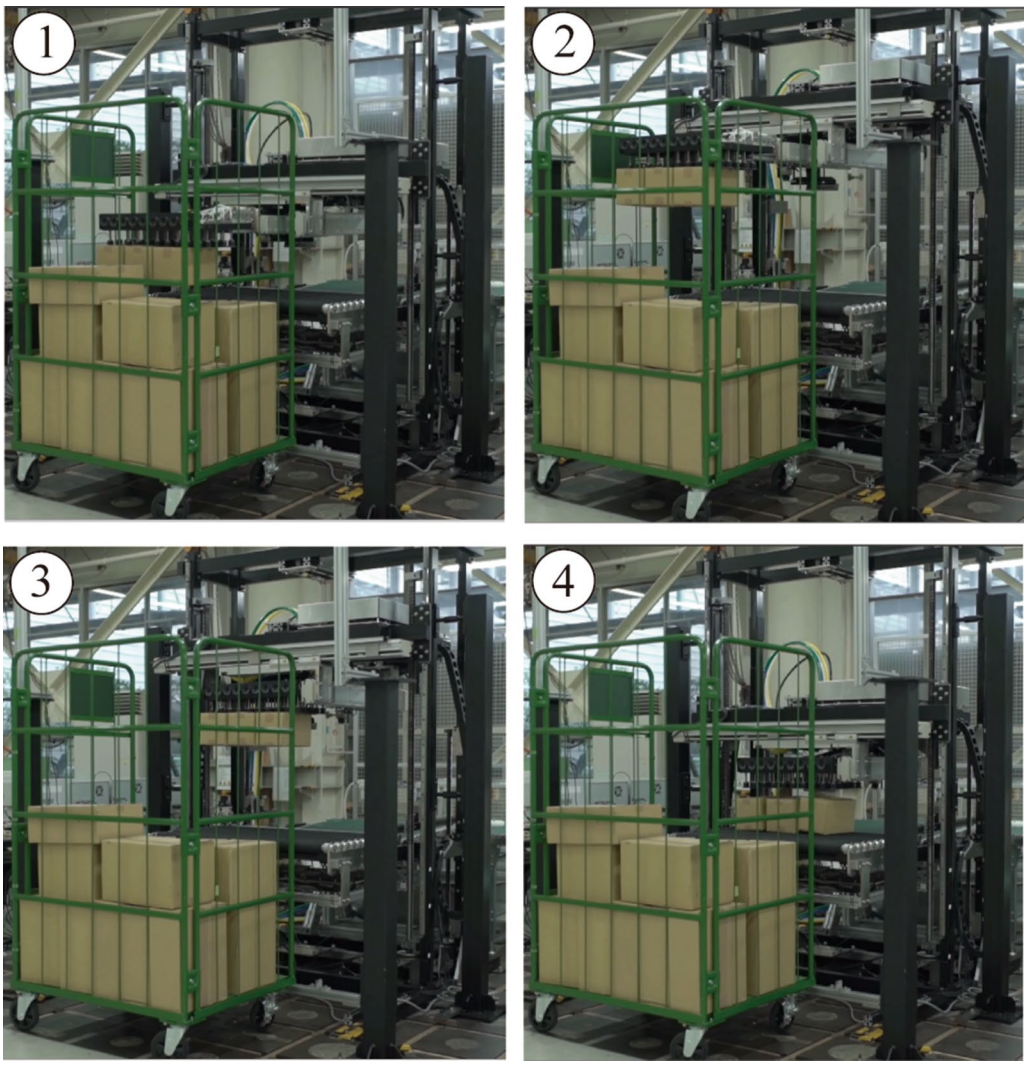


**Fig. 4** Unloading operation by a conventional linear motion-type depalletizing robot

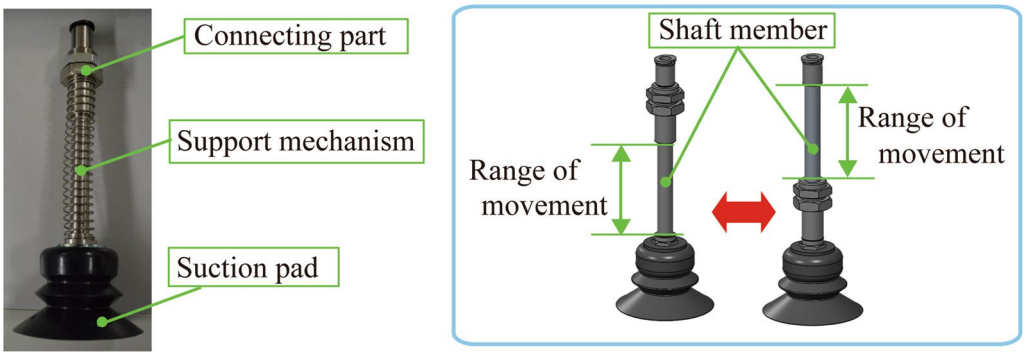


**a** Appearance **b** Expansion and contraction operation

**Fig. 5** Conventional suction pad units (VPC 50-50 BN 6 JC, PISCO). **a** Appearance, **b** expansion and contraction operation

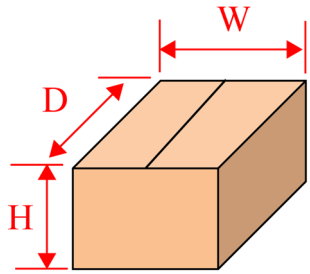


**Fig. 6** Cardboard box dimensions

**Table 1 Target cardboard boxes in the unloading operation**

| Type | W (mm) | D (mm) | H (mm) |
|---|---|---|---|
| Cardboard box ① | 280 | 380 | 255 |
| Cardboard box ② | 300 | 440 | 350 |
| Cardboard box ③ | 320 | 430 | 215 |
| Cardboard box ④ | 310 | 425 | 295 |

**Table 2 Height difference of cardboard boxes (unit (mm))**

| Type | Cardboard box ① | Cardboard box ② | Cardboard box ③ | Cardboard box ④ |
|---|---|---|---|---|
| Cardboard box ① | 0 | 95 | 40 | 40 |
| Cardboard box ② | 95 | 0 | 135 | 55 |
| Cardboard box ③ | 40 | 135 | 0 | 80 |
| Cardboard box ④ | 40 | 55 | 80 | 0 |

## Problems with conventional end effectors

Figure 7 shows a three-dimensional model for a conventional end effector using a commercially available suction pad unit [4]. A protective cover was placed on top of the end effector at the logistics site to prevent damage or contamination of the air inlet/outlet tube connected to the upper part of the suction pad unit. This protective cover is not shown in Fig. 7 to reveal the internal structure. The commercially available suction pad unit shown in Fig. 5 is 132 mm in total length, expands and contracts by 50 mm, has a 50-mm diameter suction pad, and is 80 g in mass. Therefore, as a design value, tolerance for height differences between boxes for the conventional end effector is 50 mm. When projection of the shaft member of the support mechanism and the tube fitting height are added to the suction pad unit in the initial state, the minimum height of the end effector with the protective cover is about 210 mm.

## Design principles of the proposed end effector

The development concept of the thin end effector proposed here was to realize simultaneous extraction of multiple cardboard boxes and extraction of inclined cardboard boxes with small pressing force. We considered the necessary requirements assuming a linear motion-type depalletizing robot for actual use. We considered the required performance and design principles of the end effector. To realize an end effector suitable for logistics sites, development was based on the following design principles.

### *(1) Dimensions and mass*

In the case of a roll box pallet with a middle shelf, it is desirable that workers' hands can enter the gap immediately below the middle shelf to make loading work more efficient. We therefore assumed that the gap directly beneath the middle shelf is 150 mm, and decided to reduce the thickness of the end effector, aiming at a height of less than 150 mm. Planar dimensions of the end effector were set to fit within the inner wall dimensions (W 1040 × D 1050 mm) of the roll box pallet.

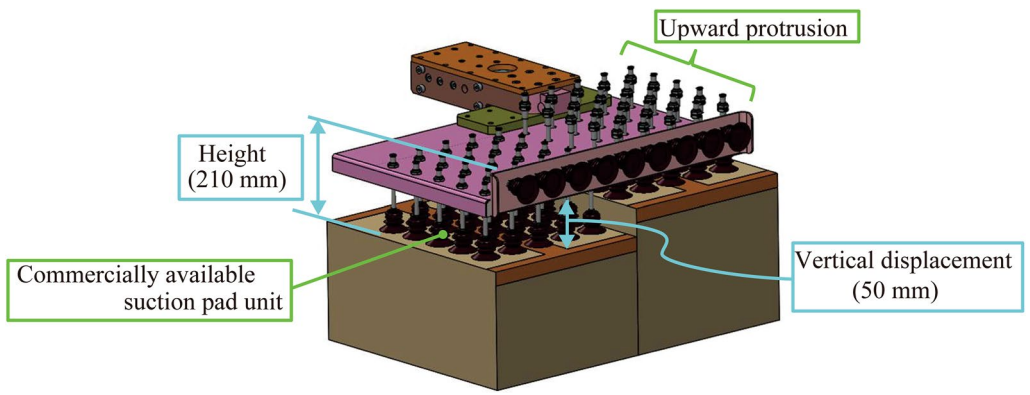


**Fig. 7** Three-dimensional diagram of a conventional end effector

The loading capacity of the main arm in linear motion-type depalletizing robots used at the time of verification was 100 kg or more. We thus decided that the mass of the end effector should not exceed 40 kg, which is the load capacity of 100 kg minus the estimated maximum load of 60 kg for two cardboard boxes.

#### *(2) Simultaneous extraction of multiple cardboard boxes*

For the end effector to simultaneously extract multiple differently sized cardboard boxes, it is necessary to allow for height difference between boxes through expansion and contraction operations of the bellows pneumatic actuator. Since the upper limit on height difference between boxes was estimated to be 80 mm, the target amount for expansion and contraction of the bellows pneumatic actuator was set at 80 mm or more.

As an expansion method to prevent expansion failure in the bellows pneumatic actuator, by making the interior of the bellows pneumatic actuator contract through decompression into atmosphere, the decompression state is canceled by airflow from the atmosphere. The bellows pneumatic actuator elongates due to air inflow and the weight of the suction pad. At the time of expansion, therefore, the suction pad can contact the upper surface of a cardboard box with a small pressing force, preventing crushing of the box.

#### *(3) Response to cardboard box collapse*

Inclination of cardboard box upper surfaces due to collapse, etc., is accommodated through flexibility of the bellows pneumatic actuator. Besides the material and shape of the suction pad, actuator flexibility as a supporting mechanism also contributes to the suction pad's ability to follow the box surface. Since inclination of the cardboard box was estimated to be 20.0°, the target allowable inclination of the box was set at 20.0° or more.

#### *(4) Contraction force*

To lift a heavy cardboard box, it is necessary to improve the contraction force generated by depressurizing the bellows pneumatic actuator. One cause of decreased contraction force is a phenomenon in which the actuator deforms in the diametrical direction without crushing in the axial direction during depressurization and crushing. Therefore, to improve the contraction force of the bellows pneumatic actuator, it should be difficult for the bellows rubber to crush in the diametrical direction during depressurization. Therefore, we considered a low-cost design that improves the contraction force of the bellows pneumatic actuator, exceeding the suction force of the suction pad.

#### *(5) Load-bearing capacity*

The bellows rubber may break if the weight of the cardboard box itself acts to expand the bellows pneumatic actuator. We therefore aimed at improving the load-bearing capacity of the bellows pneumatic actuator in the stretched state, and furthermore at a low-cost design whereby it would be difficult to inhibit bellows operation as a measure for improving load-bearing performance. The target load capacity of the bellows pneumatic actuator was to be not less than the suction force of the suction pad.

#### *(6) Unloading capacity*

Human workers can process 900 packages per hour when unloading small boxes. This is because workers can hold and transfer multiple boxes simultaneously in one unload operation. However, large boxes reduce the efficiency of unloading work. In addition, human workers need to take breaks, so the work speed gradually decreases as fatigue accumulates. In this study, we targeted relatively large cardboard boxes, and, since functioning robots can continuously operate for 24 h each day, we targeted 300 packages or more as the hourly unloading capacity.

### Overview of the developed suction pad unit

Figure 8 shows the extended state of the developed suction pad unit, and Fig. 9 shows the contracted state. The total mass of the developed suction pad unit is 267 g, its height is 230 mm in the extended state and 145 mm in the contracted state, and the difference between expansion and contraction amounts is 85 mm. The suction pad is a bellows type, and its diameter is ϕ 50 mm. The bellows pneumatic actuator, as a support mechanism, was set as an independent closed space that does not communicate with the suction pad. Each suction pad and bellows pneumatic actuator individually communicates with the pneumatic pressure source. As Fig. 9 shows, when the suction pad unit is in the contracted state, each conical member at the four corners of the suction pad unit base contacts the edge of the suction pad fixing member, so the fixing member does not move. Because of its hard structure, even if an external force due to acceleration or deceleration acts on the attracting pad unit in the contracted state, it can be expected to maintain its attitude. To improve the contraction force of the bellows pneumatic actuator, a thin ring member (inner diameter 30 mm, outer diameter 40 mm, thickness 1 mm) made of stainless steel was inserted through the opening of the bellows rubber (Fig. 10) and arranged in all the crest parts. To reduce cost, a commercial bellows rubber (Model number: FKM-4) was adopted (inner diameter 30 mm, outer diameter 46 mm, ridge count 16, minimum

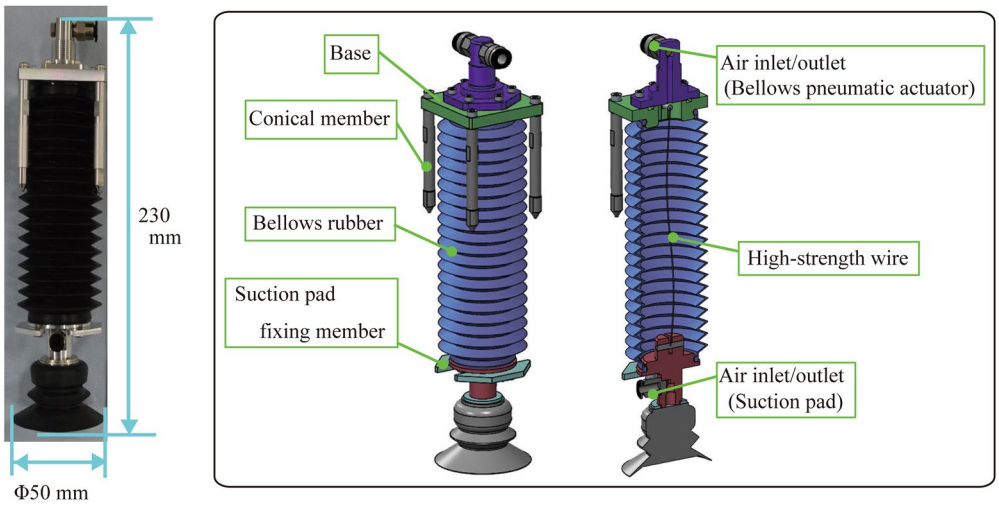


**Fig. 8** Extension state of the developed suction pad unit. **a** Actual device, **b** three-dimensional model

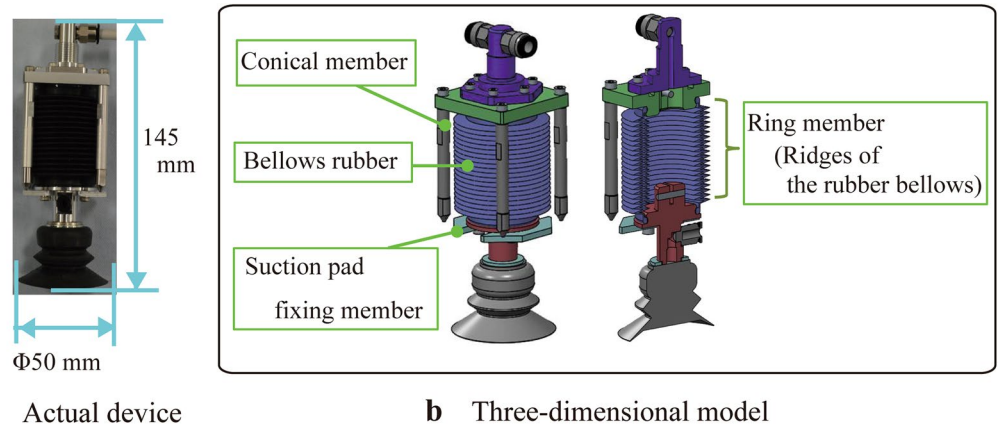


**Fig. 9** Reduction state of developed suction pad unit. **a** Actual device, **b** three-dimensional model

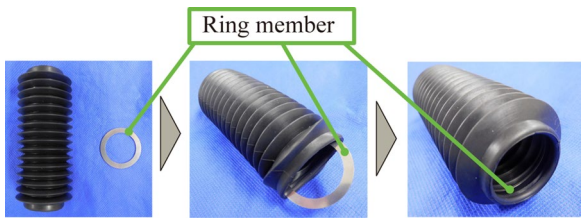


**Fig. 10** Thin ring member insertion and assembly procedure for improving contraction force of the bellows pneumatic actuator

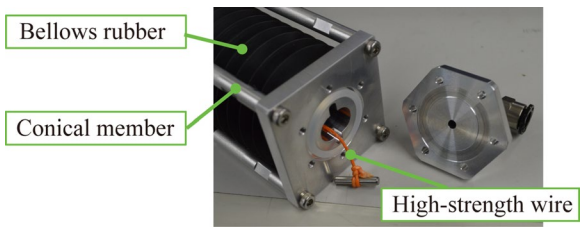


**Fig. 11** Method for improving load-bearing capacity of the bellows pneumatic actuator

length 45 mm, maximum length 140 mm). To improve the load-carrying capacity of the suction pad unit, a high-strength wire rod was placed inside the bellows rubber (Fig. 11). Ultra Dyneema 30 (strength 120 kg) fishing line was adopted as the high-strength wire. The relational expression in Eq. (1) was established between the

maximum length $l_{be\_max}$ of the bellows rubber and the maximum length $l_{ya\_max}$ of the high-strength wire rod.

$$l_{ya\_max} < l_{be\_max}. \tag{1}$$

By adjusting the wire rod length, it reached the maximum length $l_{ya\_max}$ before the bellows rubber reached the maximum length $l_{be\_max}$. As a result, the weight of the cardboard box held by the suction pad unit in the extended state acts on the high-strength wire rod instead of on the bellows rubber. In addition, although the use a metal wire with a different tensile strength is conceivable, metal wire is difficult to bend and there are concerns that the bending and the expansion and contraction of the bellows may be hindered. In consideration of flexibility, we used Ultra Dyneema 30 fishing line in this study.

Figure 12 shows a schematic diagram of the system configuration of the bellows pneumatic actuator. A directional control valve ① is connected to the suction pad switches in three states: communication between the suction pad and the vacuum pump (maximum pressure: −100 kPa), communication between the suction pad and the compressor, and communication cutoff. The suction pad either holds or releases the cardboard box as a result. The suction state of the suction pad is determined by inputting the pressure sensor value to the controller. Operation of directional control valves ① and ② at expansion and contraction of the bellows pneumatic actuator occurs as follows: Directional control valve ① is connected to the bellows pneumatic actuator and switches between two states: communication between the bellows pneumatic actuator and the vacuum pump or communication cutoff. Directional control valve ② is connected to the bellows pneumatic actuator and switches between two states: communication between the bellows pneumatic actuator and the atmosphere or cutoff of communication. During contraction of the bellows pneumatic actuator, directional control valve ② is shut off, directional control valve ① communicates with the bellows pneumatic actuator and the vacuum pump, and the vacuum pump discharges air from within the bellows pneumatic actuator. During expansion of the bellows pneumatic actuator, directional control valve ① is shut off, directional control valve ② communicates between the bellows pneumatic actuator and the atmosphere, and air flows into the bellows pneumatic actuator from the atmosphere. Damage in the entire bellows

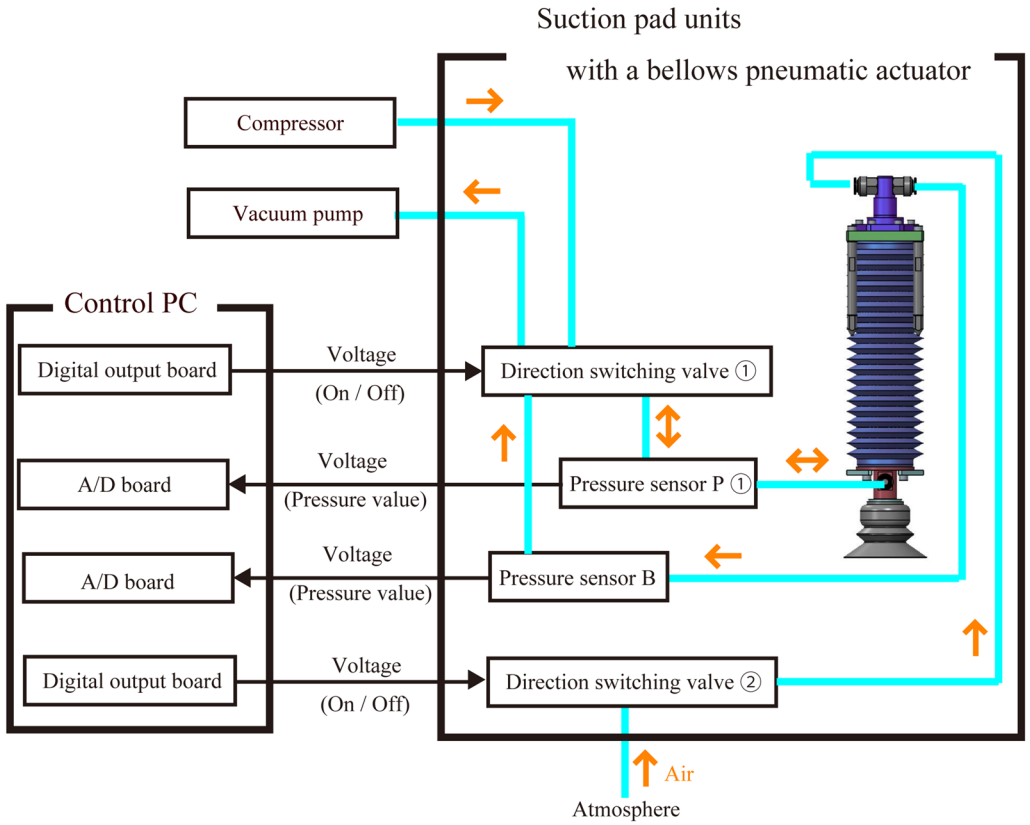


**Fig. 12** System configuration of suction pad units with a bellows pneumatic actuator

pneumatic actuator can be detected by connecting a pressure sensor to each bellows pneumatic actuator and measuring the amount of pressure change. However, it is not possible to identify damaged parts within a bellows pneumatic actuator with a metal ring. In the future, placing a sensor that detects external light on the metal ring may allow identification of damaged parts.

#### Experiment 1-1: evaluation of pressing force by a suction pad unit

We compared pressing force at the time of suction pad contact between a commercially available suction pad unit and the developed unit. Figure 13 shows the test equipment, which included a fixed part of the suction pad unit and a non-air-permeable acrylic plate as the suction target. The fixed part of the suction pad unit can be moved by manually moving the ball screw of the vertical movement mechanism. The acrylic plate can be tilted at an arbitrary angle, and is connected to a force gauge (eDPU-500N, IMADA) to measure the force.

We first describe the experimental procedure for the commercially available suction pad unit. First, we attached the connection part of the suction pad unit to the fixed part of the test device, as shown in Fig. 14a. We then pressed down on the fixed part of the test device, as shown in Fig. 14b, and measured the pressure when the spring was maximally reduced.

For the developed suction pad unit, we first attached the connection part of the unit in its reduced state to the fixed part of the test device, as shown in Fig. 15a. The distance between the suction pad and the acrylic plate is $l_{push}$. Then, as shown in Fig. 15b, the inside of the bellows communicates with the atmosphere to release the contraction state, at which point we measured the maximum pressing force by the bellows pneumatic actuator.

#### Experiment 1-2: evaluation of slope tolerance by a suction pad unit

Using the test equipment shown in Fig. 13, we measured the allowable inclination when the developed suction pad unit in the contracted state is elongated. First, as Fig. 16 shows, we put the suction pad unit in the contracted state as its initial state, then adjusted the suction pad and the acrylic plate to an arbitrary distance $l_{inc}$ and angle $\theta_{inc}$. The suction pad was then brought into a suction state by communicating with the vacuum pump. Finally, we elongated the suction pad unit through communication between the interior of the bellows pneumatic actuator and the atmosphere, and confirmed the presence or absence of suction between the suction pad and the acrylic plate. As the experimental conditions in Fig. 17 show, we obtained the maximum distance $l_{inc}$ at which the suction pad can hold the acrylic plate when the inclination angle $\theta_{inc}$ of the acrylic plate was 10°, 20°, or 30°. Further, we determined the distance $l_{bent}$ from the center of the suction pad unit connection portion to the bending portion of the bellows at the time of suction.

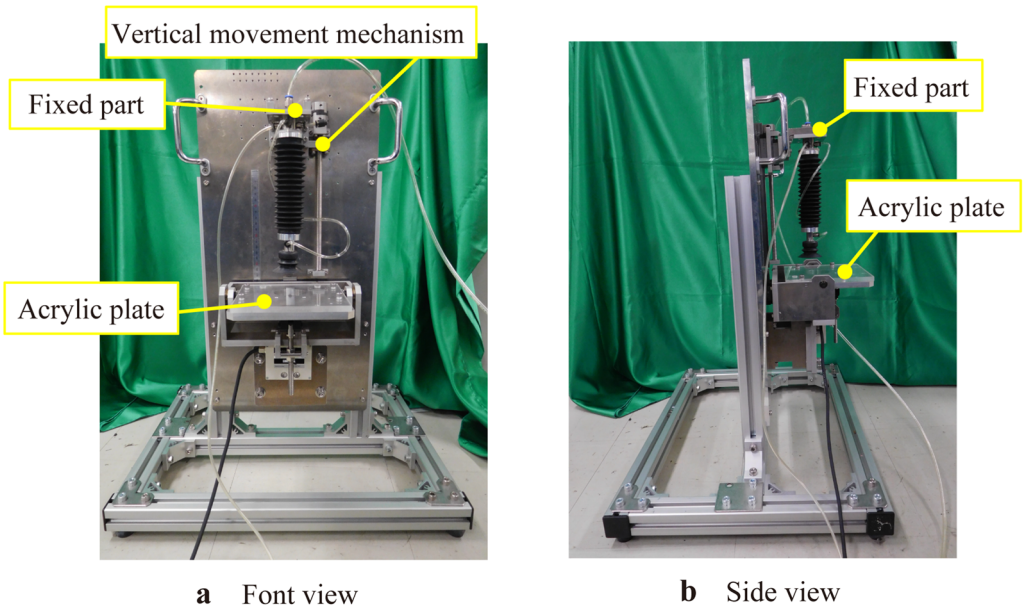


**Fig. 13** Characteristic evaluation device for the suction pad unit. **a** Front view, **b** side view. The developed suction pad unit was attached to the evaluation device

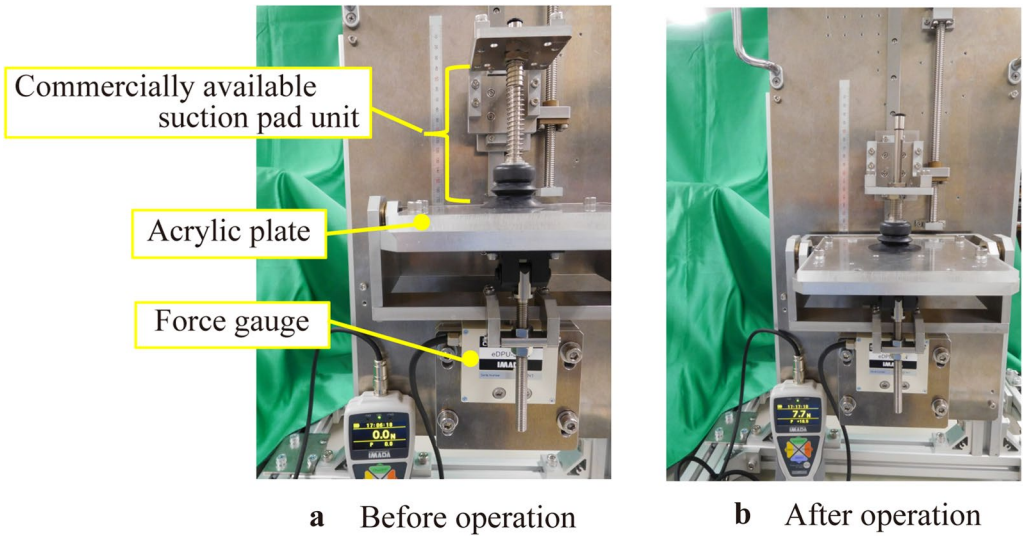


**Fig. 14** Evaluation of pressing force of a commercially available suction pad unit. **a** Before operation, **b** after operation

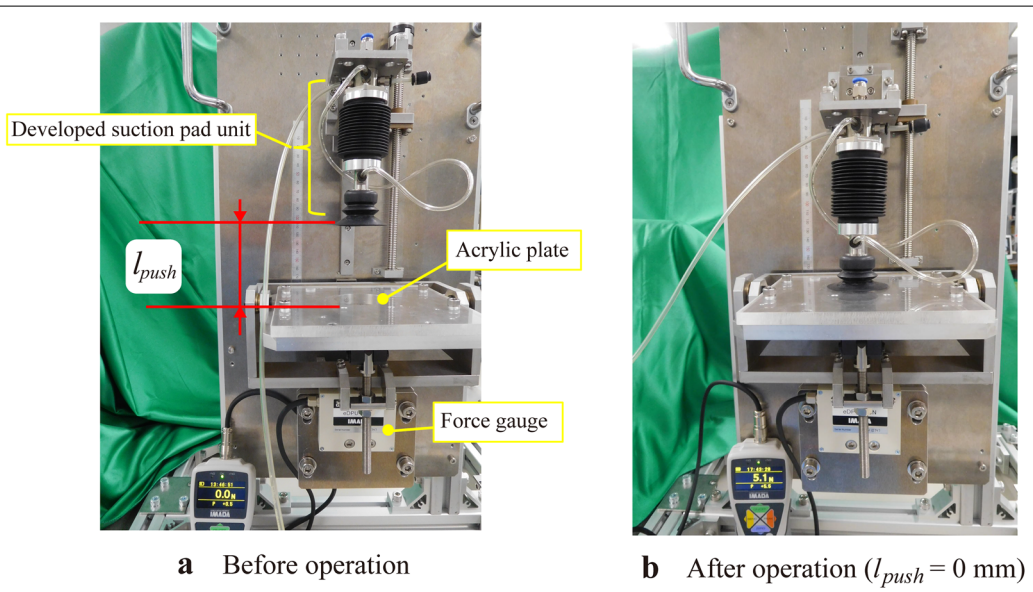


**Fig. 15** Evaluation of pressing force of the developed suction pad unit. **a** Before operation, **b** after operation ($l_{push}$ = 0 mm)

#### Experiment 1-3: evaluation of contraction force by a suction pad unit

Using the test equipment shown in Fig. 13, we measured the maximum contraction force when the developed suction pad unit in the extended state contracts. As an experimental procedure (Fig. 18), the suction pad of the extended suction pad unit was first held to the acrylic plate by suction, the distance between the fixed part of the test equipment and the acrylic plate was adjusted, and the length $l_{con}$ of the bellows pneumatic actuator was set to an arbitrary value. The maximum contraction force of the bellows pneumatic actuator was then measured by discharging the air inside the actuator with a vacuum pump. In the experiment, we set the length $l_{con}$ of the bellows pneumatic actuator to 70, 90, 110, and 130 mm, and measured the difference in contraction force due to the presence or absence of a ring member inside the bellows rubber for comparison and verification. Simply estimating the contraction force based on Pascal's principle, the relationship

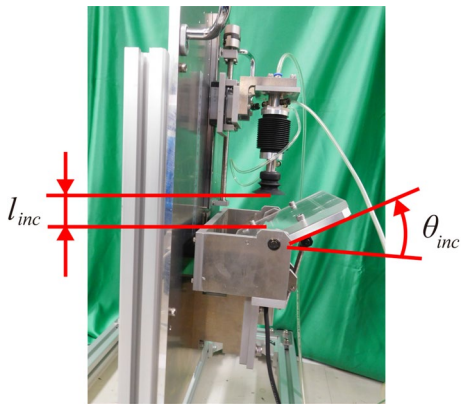


**Fig. 16** Experimental parameters for tolerance evaluation

between the pressure P (kPa), bellows rubber inner diameter D (mm), and the generated force F (N) is expressed as

$$F = \left| P \cdot \left( \frac{D}{2} \right)^2 \cdot \pi \cdot \frac{1}{1000} \right|. \quad (2)$$

When the pressure P is −100 kPa and the bellows rubber inner diameter D is 30 mm, the generated force F is about 71 N. This is lower than the calculated force due to deformation of the bellows rubber or sliding resistance between the parts.

#### Experiment 1-4: evaluation of load-bearing performance by a suction pad unit

We evaluated the load-bearing capacity of the suction pad unit in the extended state (Fig. 19). In the first step of the experimental procedure, we set the suction pad unit to the extended state. Next, we brought the suction pad into a suction state by communicating with the vacuum pump, and held a 5.5-kg weight by suction. The bellows rubber was then checked for breakage.

#### Experiment 1-5: evaluation of load and stretch length of a bellows pneumatic actuator with a ring member within the bellows

Using the test device shown in Fig. 20, we evaluated the relationship between load and displacement in the proposed bellows pneumatic actuator with a ring member within the bellows. Note that there is no high-strength wire inside the bellows pneumatic actuator. We improved the test device so that both ends of the bellows pneumatic actuator could be fixed. The lower end of the bellows pneumatic actuator is connected to a fixed plate, and the fixed plate is connected to a force gauge (IMAD eDPU-500N). The upper end of the bellows pneumatic actuator is connected to another fixing plate. The total length of the bellows pneumatic actuator can be changed by manually turning the ball screw of the vertical movement mechanism.

As shown in Fig. 20a, the natural length $l_{ini}$ (mm) of the bellows pneumatic actuator is first measured in the experimental procedure. The lower end of the bellows

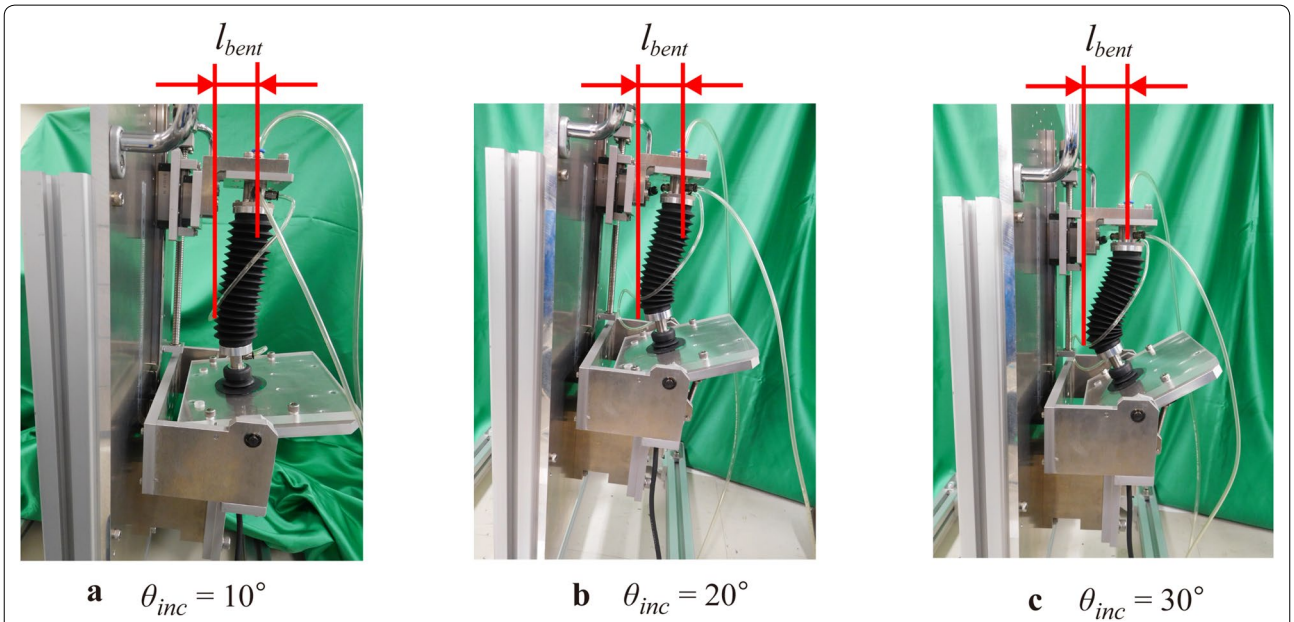


**Fig. 17** Experimental view of tolerance evaluation for tilting. **a** $\theta_{inc} = 10°$, **b** $\theta_{inc} = 20°$, **c** $\theta_{inc} = 30°$

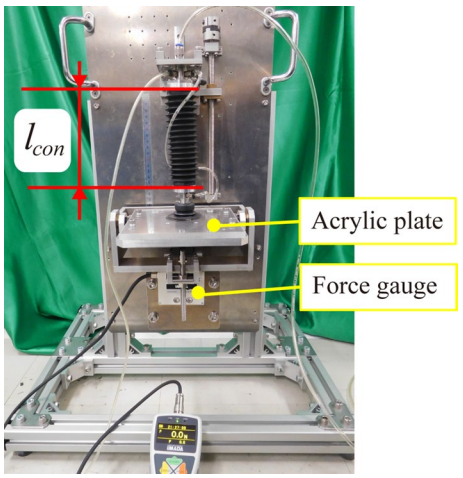


**Fig. 18** Experimental parameters for contractile force evaluation

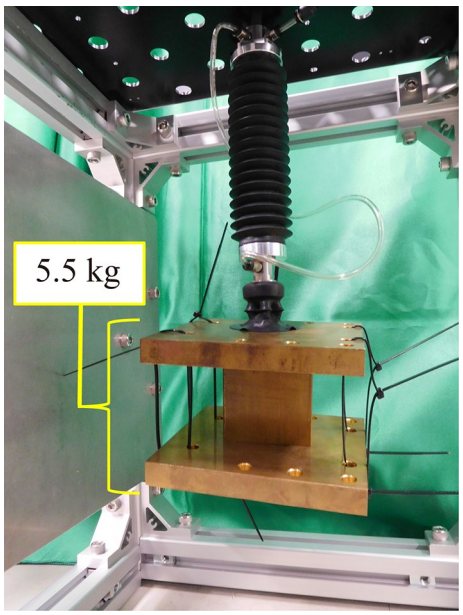


**Fig. 19** Evaluation experiment of load-bearing performance

pneumatic actuator is then connected to the fixed plate. Finally, as shown in Fig. 20b, the bellows pneumatic actuator is extended from its natural length by manually turning the ball screw of the vertical movement mechanism, and the length $l_{load}$ (mm) of the bellows pneumatic actuator and the force $F_{pull}$ (N) acting on the force gauge are measured. Here, the extension amount $l_{diff}$ of the bellows pneumatic actuator, which is the difference between the length $l_{load}$ of the bellows pneumatic actuator and the natural length $l_{ini}$, expressed as

$$l_{diff} = l_{load} - l_{ini}. \tag{3}$$

In the experiment, we measured force $F_{pull}$ acting on the force gauge under nine extension amounts $l_{diff}$ of the bellows pneumatic actuator: 0, 5, 10, 15, 20, 25, 30, 35, and 40 mm.

### Overview of the developed end effector

This section presents the detailed structure of the proposed end effector with multiple suction pad units. The end effector was attached to the main arm of the linear motion-type depalletizing robot for mechanical verification.

Figure 21 shows a three-dimensional diagram of the developed end effector. We set the planar dimensions of the end effector to W 900 mm and D 450 mm, in consideration of the design principle described. When the protective cover is in position, the height of the end effector is 145 mm in the bellows-contracted state, and the allowable height difference between cardboard boxes is 85 mm as the design value. A maximum of 50 suction pad units can be arranged on the end effector. Five suction pad units can be arranged at intervals of 60 mm in the depth direction, and ten units at intervals of 70 mm in the width direction. Also, the total mass of the end effector is about 21.5 kg.

As Fig. 22 shows, the developed end effector is attached to the main arm of a conventional linear motion-type depalletizing robot. To stably move the cardboard boxes on the belt conveyor of the conveyor arm, a follower conveyor that rocks and follows the conveyor arm's up–down movement is provided. As shown in Table 3, the structure of the drive shaft of the depalletizing robot has five degrees of freedom.

Figure 23 shows an outline of the configuration of the drive control system for the end effector. The system configuration of the end effector in Fig. 23 which differs from that of the suction pad unit in Fig. 12 has directional control valves ① and ② per five bellows pneumatic actuators. By serially connecting the flow paths of the five bellows pneumatic actuators, fewer directional control valves are required, reducing cost. As Fig. 24 shows, we confirmed basic expansion and contraction motions of each suction pad unit. Since the bellows pneumatic actuator is contracted in the hold operation, the upward movement amount of the main arm is reduced.

### Experiment 2-1: evaluation of expansion and contraction by end effector alone

We measured expansion and contraction operation times and amounts of the suction pad unit of the end effector. We evaluated these operation times with the unit actually incorporated into the linear motion-type depalletizing

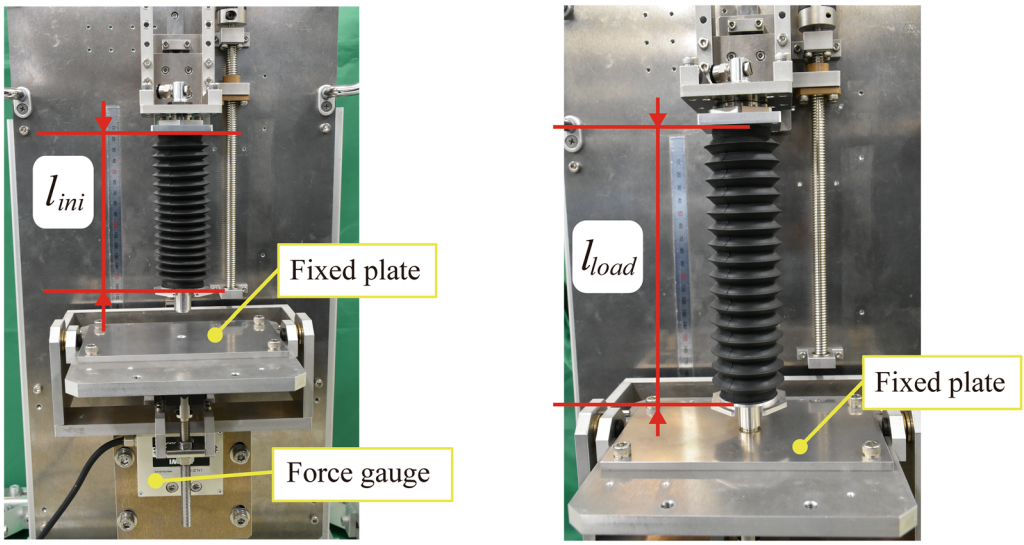


**Fig. 20** Experiment of load and stretch length of the bellows pneumatic actuator with a ring member inside. **a** Natural length state, **b** stretched state

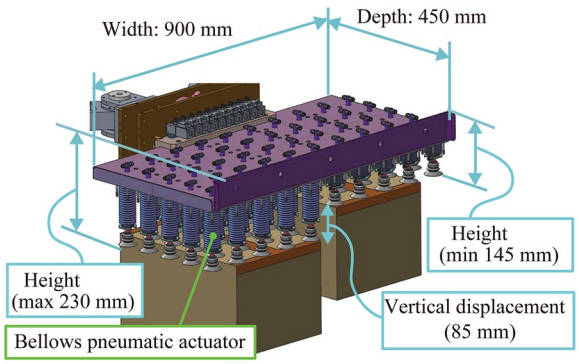


**Fig. 21** Three-dimensional diagram of the developed end effector

robot, considering loss due to the air inflow–outflow tubes. Figure 25 shows the state of the experiment, and Fig. 26 shows an outline of the configuration of the experimental system. In the experiment, the bellows pneumatic actuator in the expanded state contracts and expands, and the series of actions to be measured is implemented.

When measuring the maximum expansion and contraction operation times, we measured the suction pad units ① and ② with the longest tube paths. The tube length from the vacuum pump and the compressor to directional control valve ① was 5100 mm, that from directional control valve ① to the bellows pneumatic actuator of suction pad unit ② was 2500 mm, and that from directional control valve ② to the bellows pneumatic actuator of suction pad unit ② was 600 mm. The bellows pneumatic actuator of suction pad units ① and ② correspond to both ends of a configuration in which the tubes are connected in series. In the experimental system in Fig. 25, we placed a laser displacement sensor (IL-300, KEYENCE) directly beneath the suction pad to measure the amount of expansion and contraction. The resolution of the laser displacement sensor is 30 μm and the measurement range is up to 290 mm. To improve the accuracy of distance measurements by the laser displacement sensor, the suction pad holds in advance the corrugated board to which the reflective seal for the laser is attached. In addition, to acquire the drive command timing for the expansion and contraction motions of the suction pad unit from the controller, we used a data logger to obtain the operation command voltage input to directional control valves ① and ②.

#### Experiment 2-2: evaluation of allowable height difference between cardboard boxes by the end effector alone

The experiment shown in Fig. 27 evaluated tolerance in height differences between cardboard boxes. Testing was conducted with the operator visually confirming the position and orientation of the cardboard box and operating the up–down movement of the main arm. The boxes used in this experiment had dimensions W 410 × D 470 × H 400 mm and mass 2 kg. In the experiment, two

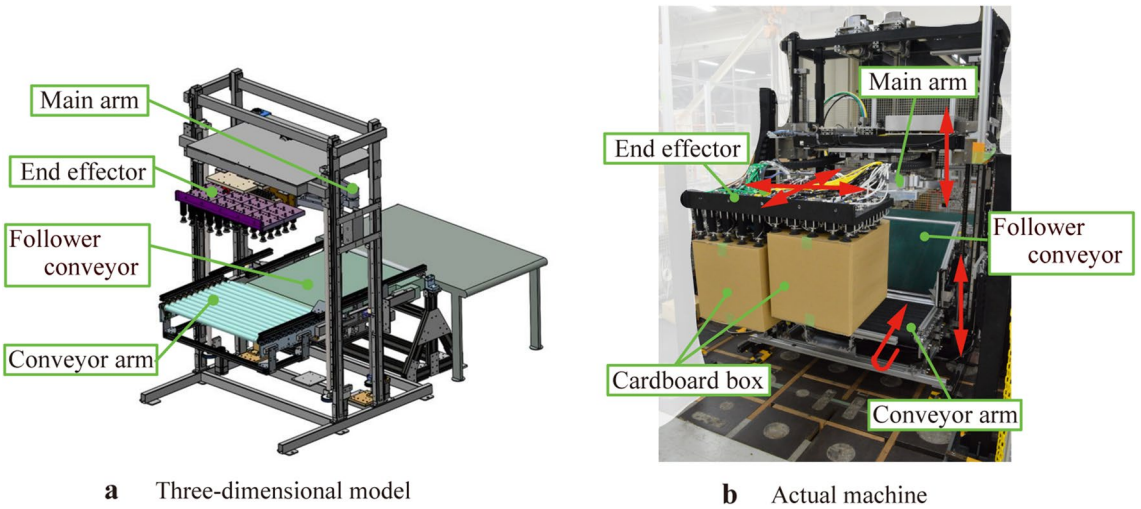


**Fig. 22** Conventional linear-motion type depalletizing robot with the developed end-effector. **a** Three-dimensional model, **b** actual machine

**Table 3 Linear motion-type depalletizing robot drive axis configuration and drive amount**

| Name | Drive axis configuration | Drive amount |
|---|---|---|
| Main arm | Three degrees of freedom | (Front and rear directions) 1170 mm |
| | | (Left–right directions) 200 mm |
| | | (Up–down directions) 1050 mm |
| Conveyor arm | Two degrees of freedom | (Up–down directions) 930 mm |
| | | Drive endless rotation of belt conveyor |

boxes were arranged so that the upper surface of one was higher than the other. Experimental conditions set height differences of 65, 75, and 85 mm. Height differences were initially set to an arbitrary value. The main arm was then lowered until the suction pad contacted the upper surface of one box. Thereafter, the bellows pneumatic actuator was extended. Finally, the bellows pneumatic actuator contracts and the main arm is raised to lift the box held by the suction pads. Suction hold was considered successful if both boxes were raised.

#### Experiment 2-3: evaluation of tilt tolerance of cardboard boxes by the end effector alone

The experiment shown in Fig. 28 evaluated the inclination allowance for cardboard boxes. Testing was conducted with the operator visually confirming the position and orientation of the cardboard box and operating the up–down movement of the main arm. The boxes used in this experiment had dimensions W 410 × D 470 × H 400 mm, and mass 2 kg. The upper box surface was set to an arbitrary inclination angle by adjusting the interval between two block materials on the placement surface. The experimental conditions for inclination angle of the upper box surface were 10°, 20°, and 30°. The box inclination was first set to an arbitrary value. Next, the suction pad unit was placed in a suction state through communication with the vacuum pump, and the main arm was lowered until part of the suction pads came into contact with the upper surface of the inclined box. Thereafter, the bellows pneumatic actuator was elongated so that each suction pad was brought into contact with the upper surface of the inclined box, and the box was held. Finally, the bellows pneumatic actuator contracted and the main arm was raised to lift the box held by the end effector. Suction hold was considered successful if the box was raised.

#### Experiment 2-4: evaluation of contraction force by the end effector alone

We evaluated the relation between the number of suction pad units on the end effector acting on the cardboard box and the contraction force. Testing was conducted with the operator visually confirming the position and orientation of the cardboard box and operating the up–down movement of the main arm. The boxes used for this experiment had dimensions W 410 × D 470 × H 400 mm. As Fig. 29 shows, the experimental apparatus was constructed by setting a plate member on the bottom surface inside the box and connecting the plate member to a load cell (eDPU-5000N, IMADA). In the first step of the experiment, the box was fixed to the test apparatus. Next, the suction pad unit is placed in an extended state, and the upper surface of the box is held by the suction pads. Then, the

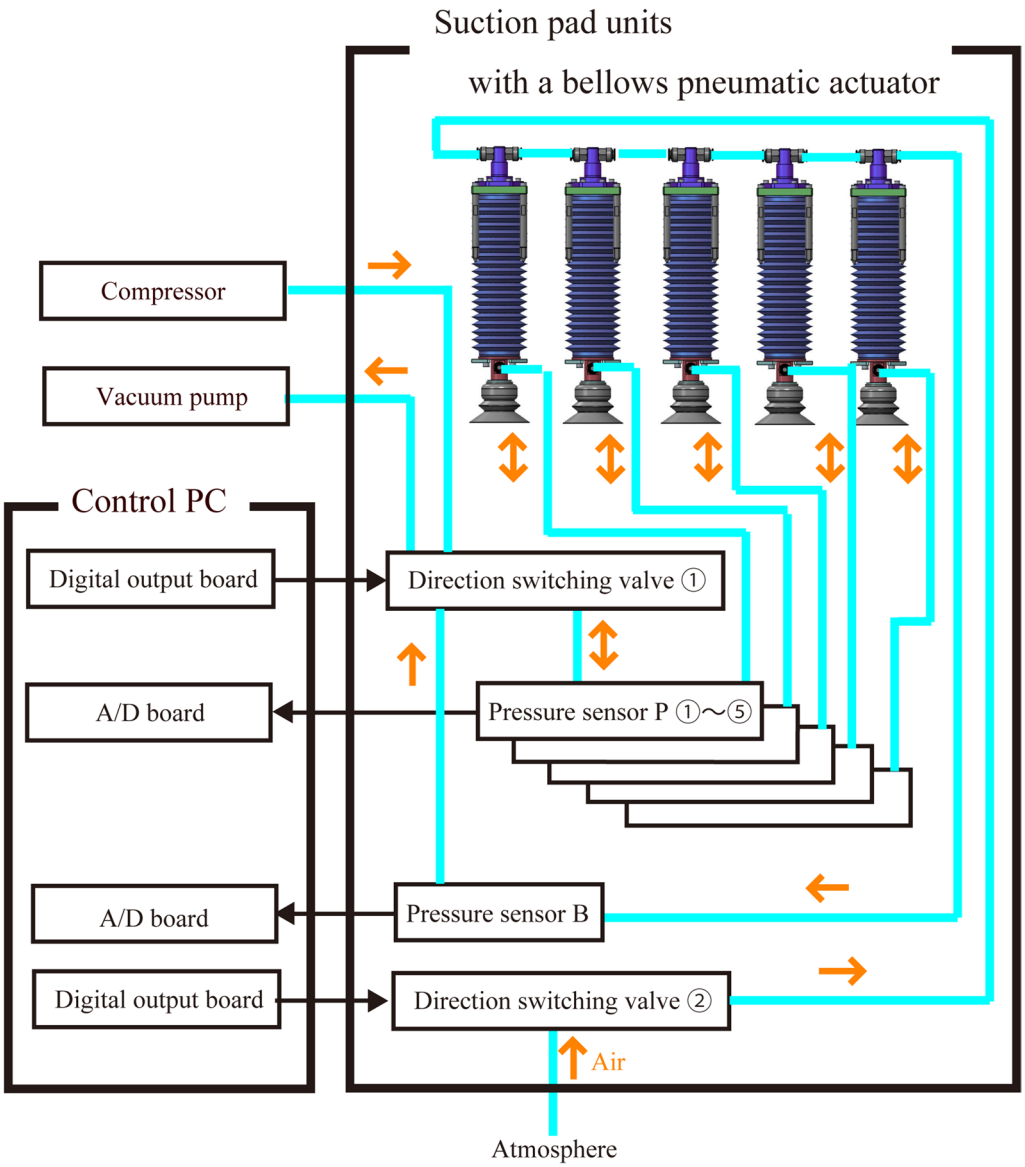


**Fig. 23** Configuration of the drive control system for the developed end effector

bellows pneumatic actuator contracts with the main arm in the servo lock state. Experimental conditions set the number of used suction pad units to 5, 10, 15, 20, 25, and 30.

#### Experiment 2-5: continuous transfer evaluation

This section describes the experimental results for a series of unloading operations performed by a linear motion-type depalletizing robot. In these experiments, we used a distribution warehouse roll box pallet without a middle shelf.

To measure the position and orientation of cardboard boxes on a roll box pallet, we placed an RGB-D camera on the linear motion-type depalletizing robot. Figure 30 shows an example of the measurement results. As a safety measure to prevent the end effector from crushing a cardboard box due to RGB-D camera measurement error, the positioning target value of the end effector was set to 10 mm above the measurement result for the top of the box. The main arm needs to return to its initial posture so as not to block the field of view of the RGB-D camera each time the box position and posture are measured. The linear motion-type depalletizing robot operates based on commands from a controller. Figure 31 shows the rough flow of motion

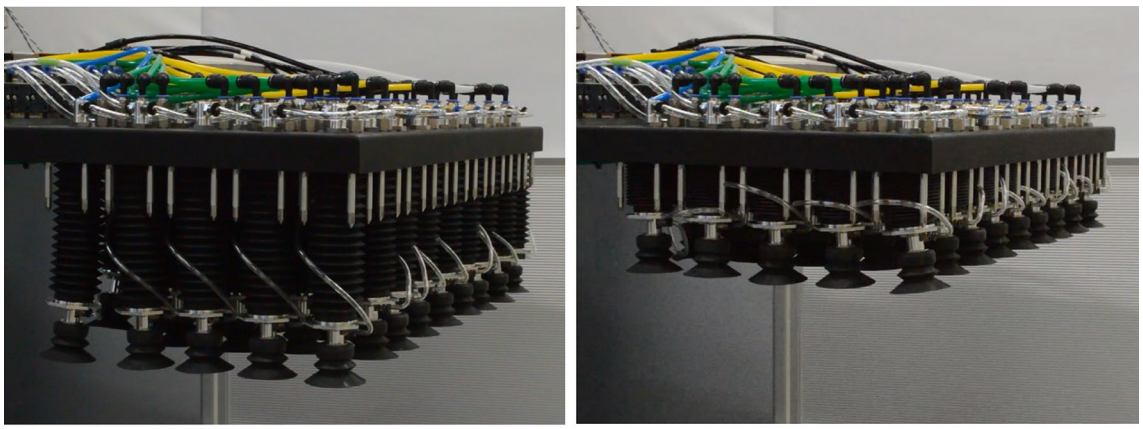


**Fig. 24** Basic expansion and contraction motions of each suction pad unit of the end effector. **a** Expansion, **b** contraction

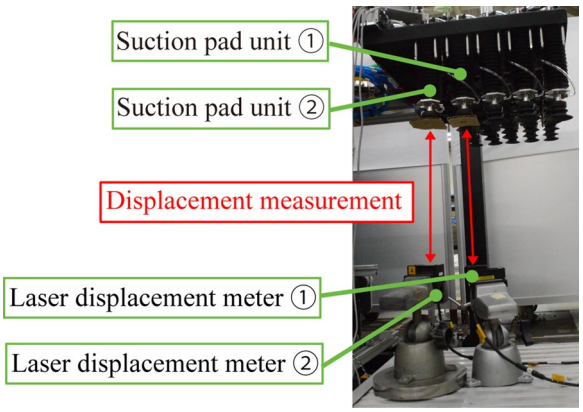


**Fig. 25** Expansion and contraction motion evaluation experiment for the end effector

processing, and Fig. 32 shows an operation schematic diagram for each motion.

The linear motion-type depalletizing robot measured each operation time when 16 cardboard boxes were continuously extracted from the roll box pallet. At this time, boxes of different sizes were mixed and placed in a loaded state in the roll box pallet. To quantify the unload operation, a default box was placed in the roll box pallet in a predetermined loading pattern, shown in Fig. 33. Table 4 shows the box types, and Fig. 34 shows the state of one part of the verification experiment. Figure 35 shows how two boxes are simultaneously removed, with the conveyor arm moving upward and the follower conveyor also inclining so it blocks the field of view of the shooting screen. Note that the bottom box ⑤ is for height adjustment of the other boxes and is not unloaded. As part of this experiment, we measured operation times for extracting each box from the roll box pallet.

## Results

### Results of experiment 1-1: evaluation of pressing force by the suction pad unit

We found that the maximum pressing force of the commercially available suction pad unit was about 7.7 N. As Fig. 36 shows, the maximum pressing force of the developed suction pad unit was about 5.1 N. This confirmed that the developed suction pad unit had a smaller pressing force than did the commercially available unit.

As Fig. 36 shows, when distance $l_{push}$ (mm) of the developed suction pad unit changes in a range of 0 to 75 mm, the maximum pressing force $F_{push}$ (N) is the approximate polynomial in Eq. (4).

$$F_{push} = -0.00003l_{push}^3 + 0.0036l_{push}^2 - 0.188l_{push} + 4.7369. \quad (4)$$

At this time, the coefficient of determination $R^2$ is 0.9816. In the developed suction pad unit, the maximum pressing force $F_{push}$ (N) decreases as the distance $l_{push}$ (mm) increases. Therefore, the cardboard box is less likely to be crushed as the suction pads extend further from the top surface of the cardboard box.

### Results of experiment 1-2: evaluation of slope tolerance by the suction pad unit

Table 5 shows the results of the experiment, which confirmed that the developed suction pad unit can tolerate the targeted inclination of 20° or more. When the distance $l_{inc}$ becomes large, a gap forms between the surface of part of the suction pad and the acrylic plate, and

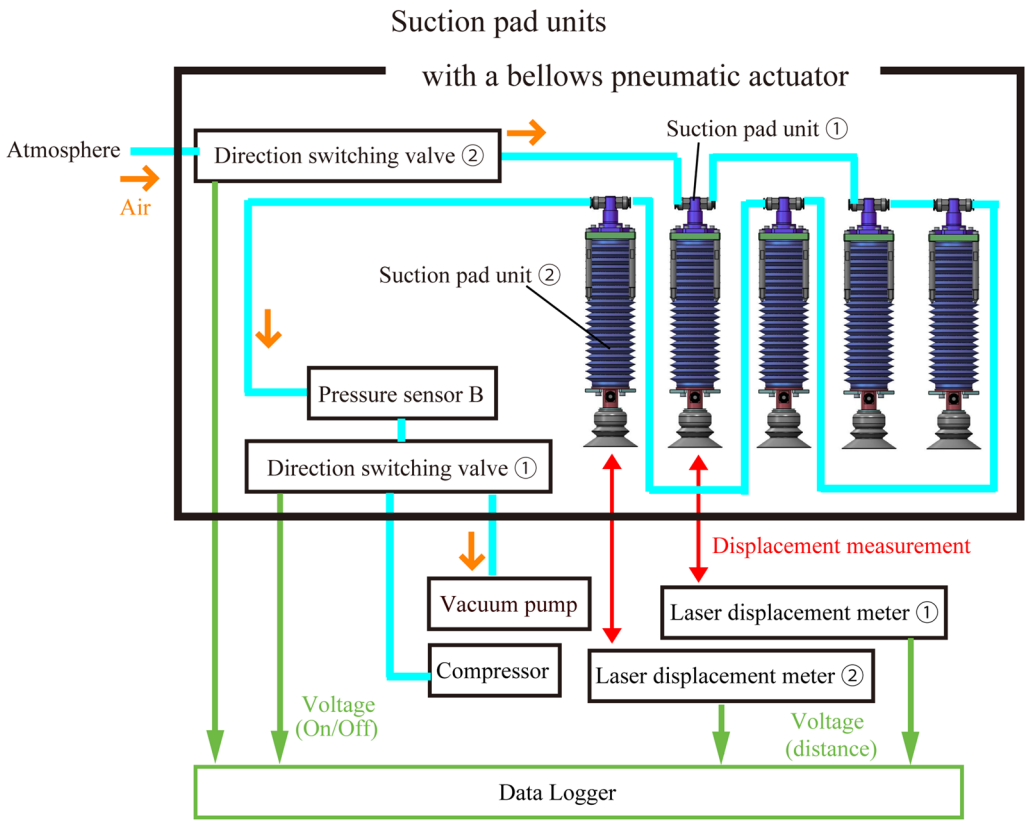


**Fig. 26** Configuration of the expansion and contraction motion evaluation experiment system

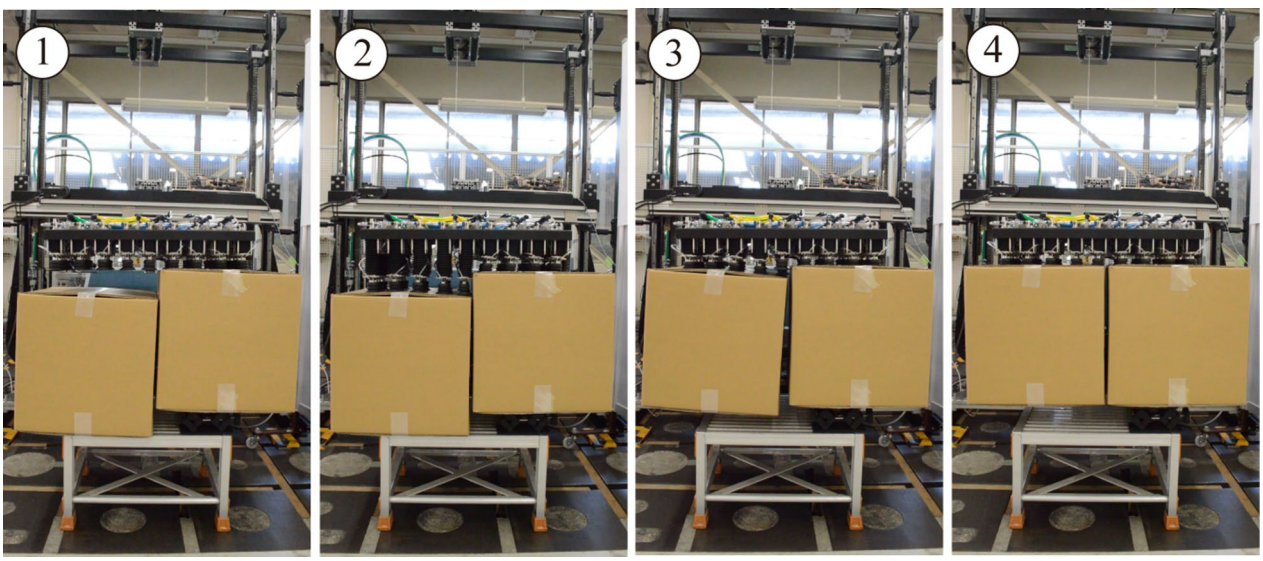


**Fig. 27** Experimental situation for cardboard boxes with height differences: 85 mm

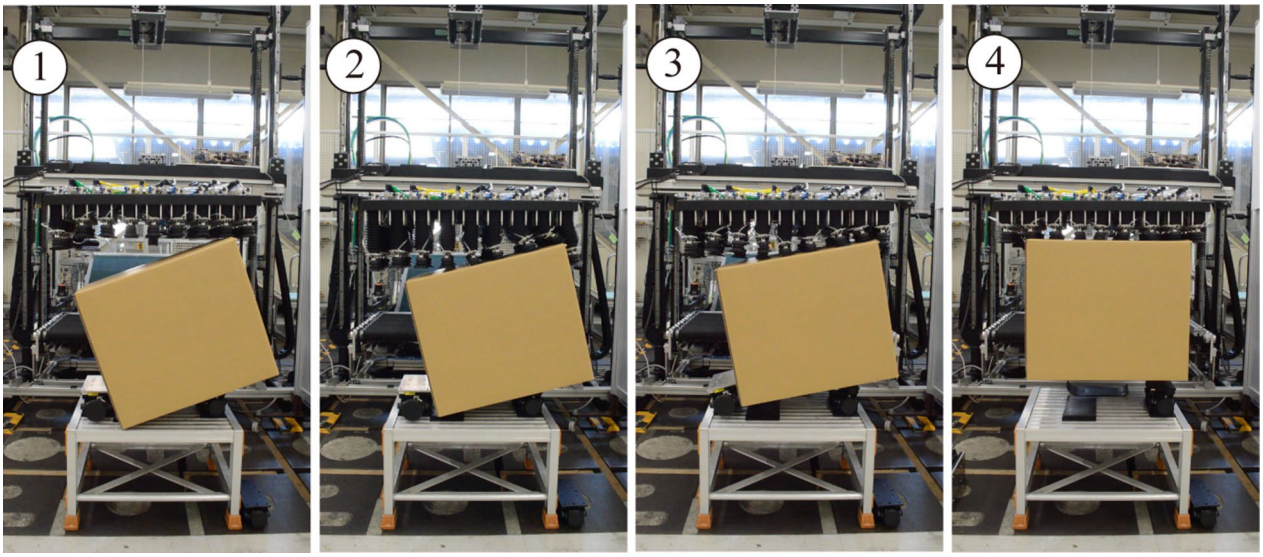


**Fig. 28** Experimental situation when tilted 20°

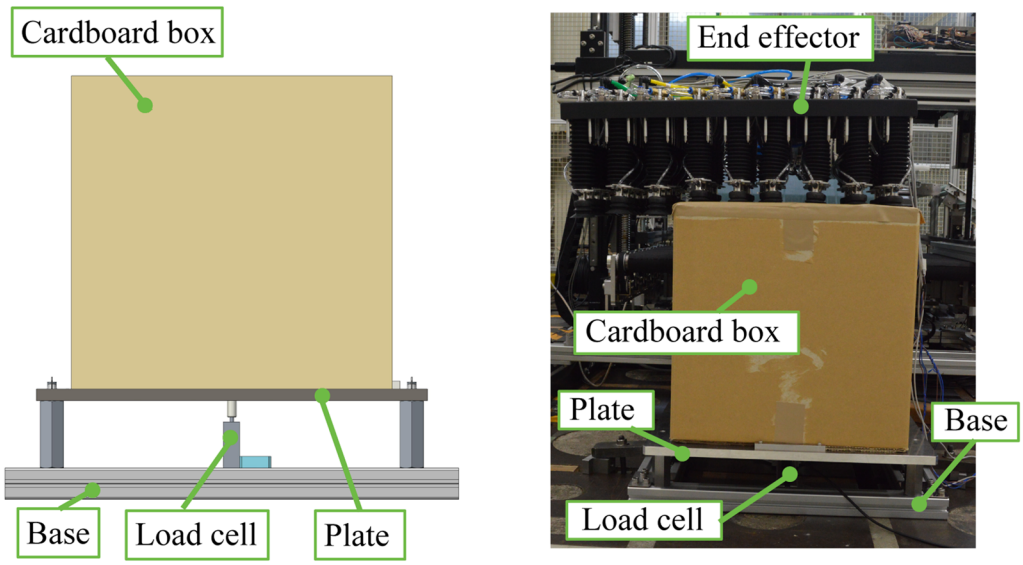


**Fig. 29** Contraction force evaluation test apparatus for the end effector alone. **a** Three-dimensional model, **b** actual experiment

the plate cannot be held by suction. In the developed suction pad unit, we confirmed that the suction pad follows the inclined surface by bending of the bellows pneumatic actuator. Further, from the measurement result of the distance $l_{bent}$, it is considered desirable that each suction pad unit be disposed on the end effector with an interval of 40 mm or more.

#### Results of experiment 1-3: evaluation of contraction force by the suction pad unit

Figure 37 shows the experimental results. As Fig. 38a shows, the bellows rubber in the configuration without a ring member collapsed in the radial direction, so the maximum contraction force was about 11–13 N. On the other hand, in the configuration with the ring member (Fig. 38b), the bellows rubber did not collapse in the radial direction,

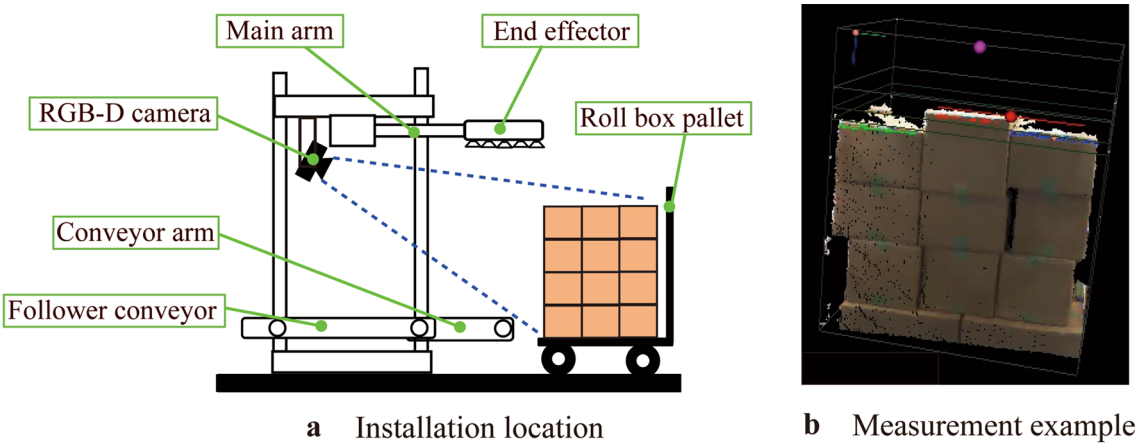


**Fig. 30** Example of measurement results by RGB-D camera. **a** Installation location, **b** measurement example

so the maximum contraction force was about 40–48 N. In the configuration with a ring member, since the contraction force exceeds the suction force of the suction pad, the suction pad moved away from the upper surface of the acrylic plate. Figure 39 shows the deformation process during the experiment when metal rings were placed inside the bellows. If metal rings are placed inside the bellows, the bellows will not collapse in the radial direction, which can prevent dramatic collapse of the bellows.

We thus confirmed that the presence or absence of the ring member inside the bellows rubber resulted in about a fourfold difference in contraction force, suggesting the possibility of lifting a cardboard box with the target maximum mass of 30 kg through the contraction force of eight or more suction pad units. Regardless of the presence or absence of the ring member, the contraction force tends to increase as the length $l_{con}$ of the bellows pneumatic actuator shortens. This is due to the smaller deformation of the bellows rubber.

#### Results of experiment 1-4: evaluation of load-bearing performance by the suction pad unit

The results confirmed that the expanded state can be maintained without breaking the bellows rubber with a 5.5-kg weight held by suction. In some cases, however, the suction pad could not maintain the holding state and dropped the weight after a period of time. This confirmed that the strength of the wire rod inside the bellows exceeded the suction force.

#### Results of experiment 1-5: evaluation of load and stretch length of the bellows pneumatic actuator with a ring member inside the bellows

Figure 40 shows the experimental results of load and stretch length for the proposed bellows pneumatic actuator with a ring member inside the bellows. Note that there is no high-strength wire inside the bellows pneumatic actuator. In Fig. 40, the horizontal axis shows the force $F_{pull}$ (N) acting on the force gauge, and the vertical axis shows the extension amount $l_{diff}$ (mm) from the natural length $l_{ini}$ (mm) of the bellows pneumatic actuator. When the extension amount $l_{diff}$ (mm) of the bellows pneumatic actuator is in a range of 0 mm to 40 mm, the following linear approximation is established between the force $F_{pull}$ (N) and the extension amount $l_{diff}$ (mm) of the bellows pneumatic actuator:

$$l_{diff} = 35.7F_{pull}. \tag{5}$$

At this time, $R^2 = 0.9707$. From Eqs. (3) and (5), the relational expression between length $l_{load}$ (mm) and natural length $l_{ini}$ (mm) of the bellows pneumatic actuator is

$$l_{load} = 35.7F_{pull} + l_{ini}. \tag{6}$$

The natural length $l_{ini}$ (mm) of the bellows pneumatic actuator was 123 mm. According to the product catalog, the maximum safe length of the bellows (model FKM-4) is 140 mm. As Eq. (1) shows, it is necessary to adjust the maximum length of the bellows pneumatic actuator and the length of the high-strength wire inside the bellows pneumatic actuator in consideration of the safe use range.

#### Results of experiment 2-1: evaluation of expansion and contraction by the end effector alone

Figure 41 shows the measurement results. In the graph in that figure, the horizontal axis is time, the left vertical axis is the displacement amount of the suction pad units as measured by laser displacement sensors ① and ②, and the right vertical axis is the operation command voltage from

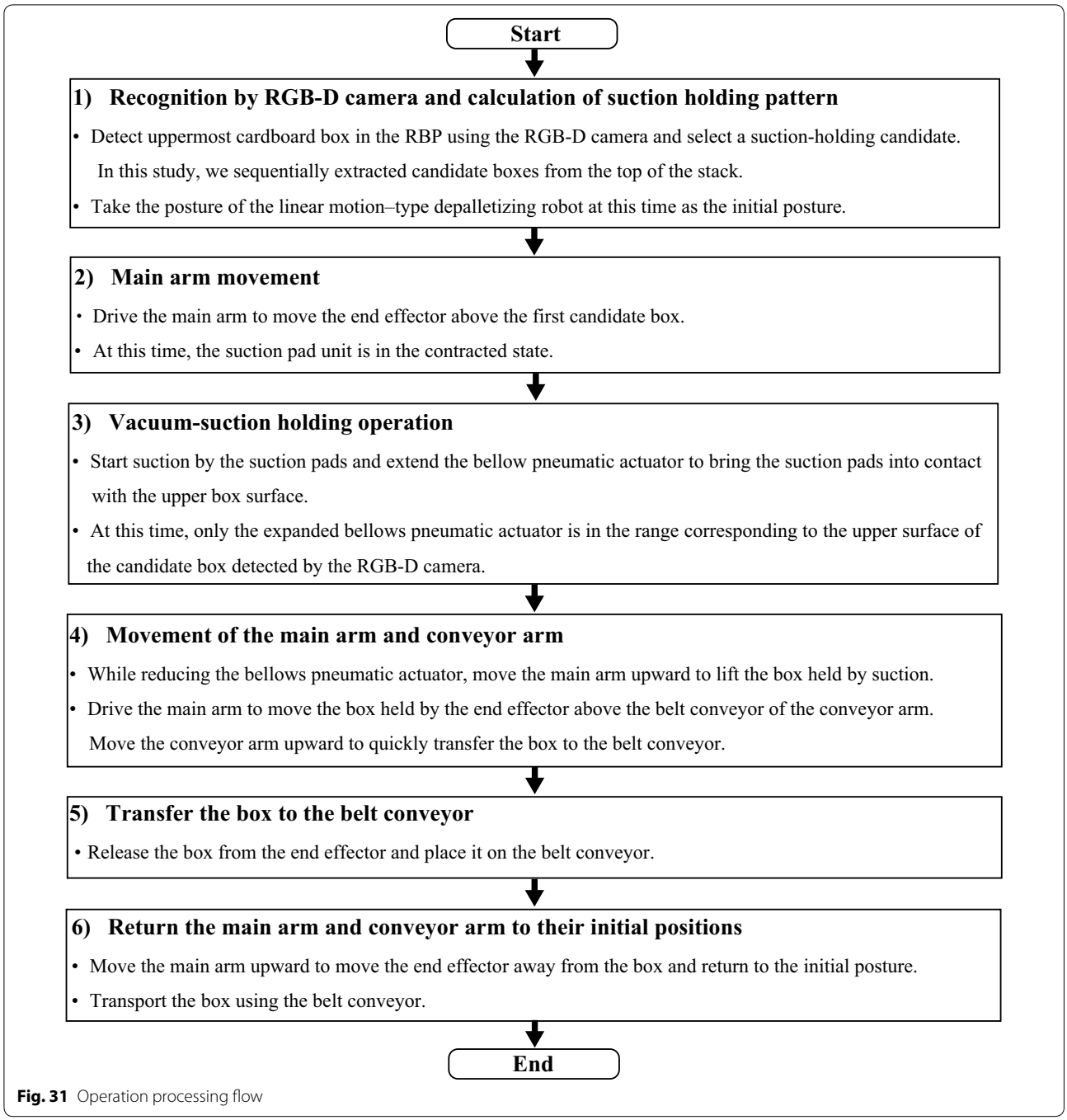


**Fig. 31** Operation processing flow

the controller input to directional control valves ① and ②. The results revealed that the contraction time for transition from the stretched state to the contracted state was about 2.70 s, and the expansion time for transition from the contracted state to the stretched state was about 7.25 s. There was no significant difference between the start timing of the expansion and contraction operations. The expansion and contraction amounts of bellows pneumatic actuators ① and ② were 85 and 80 mm, respectively.

From linear approximation, Eq. (7) gives the relationship between the expansion and contraction amount $l_{ext1}$ (mm) for suction pad unit ① and the expansion time $t_{ext}$ (s) in the range of 0 s to 7.25 s.

$$l_{ext1} = 11.7 t_{ext}. \tag{7}$$

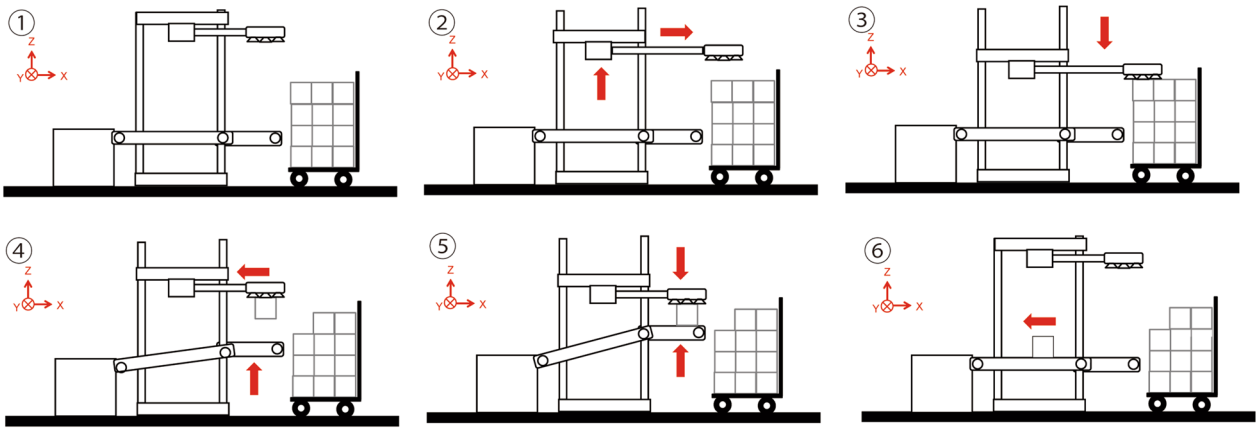


**Fig. 32** Operating procedure of unloading operations by the linear motion-type depalletizing robot

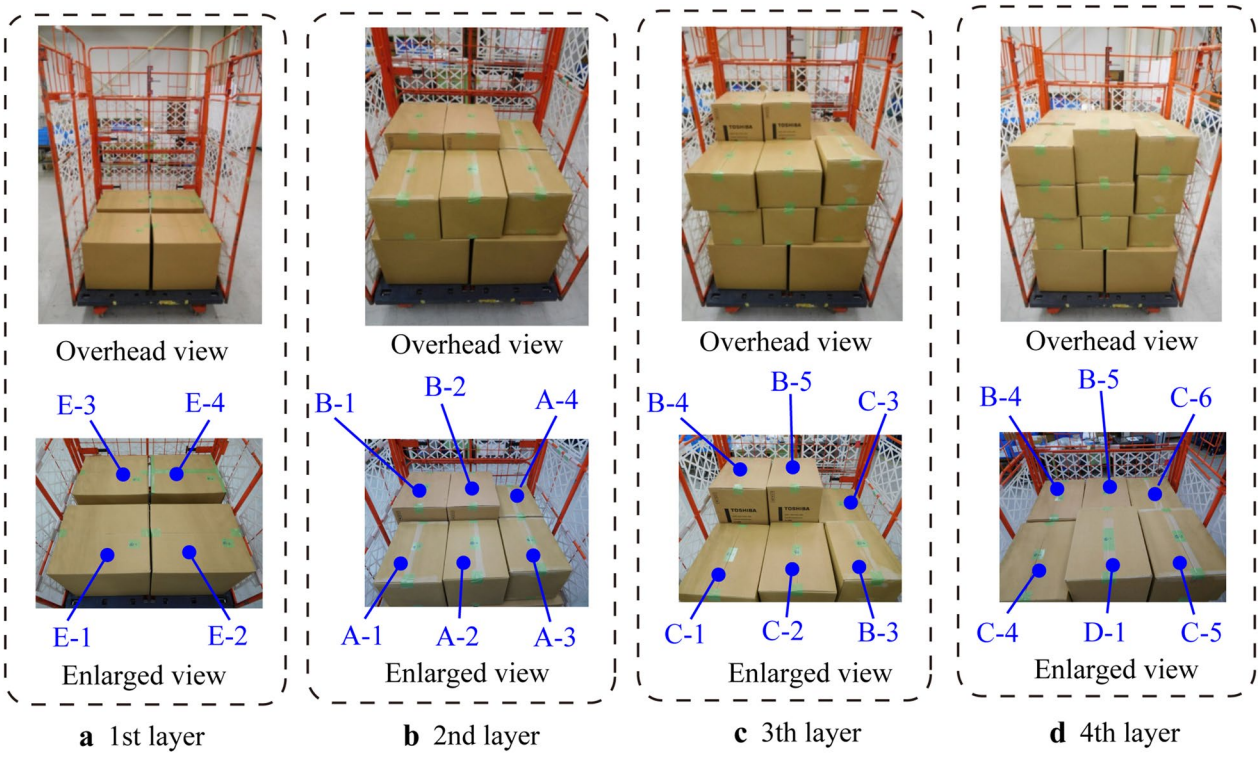


**Fig. 33** Loading pattern for cardboard boxes

**Table 4 Types of cardboard boxes**

| Type | W (mm) | D (mm) | H (mm) | Number | Notation |
|---|---|---|---|---|---|
| Cardboard box ① | 280 | 380 | 255 | 4 | A-1, A-2, A-3, A-4 |
| Cardboard box ② | 300 | 440 | 350 | 5 | B-1, B-2, B-3, B-4, B-5 |
| Cardboard box ③ | 320 | 430 | 215 | 6 | C-1, C-2, C-3, C-4, C-5, C-6 |
| Cardboard box ④ | 310 | 425 | 295 | 1 | D-1 |
| Cardboard box ⑤ | 410 | 470 | 400 | 4 | E-1, E-2, E-3, E-4 |

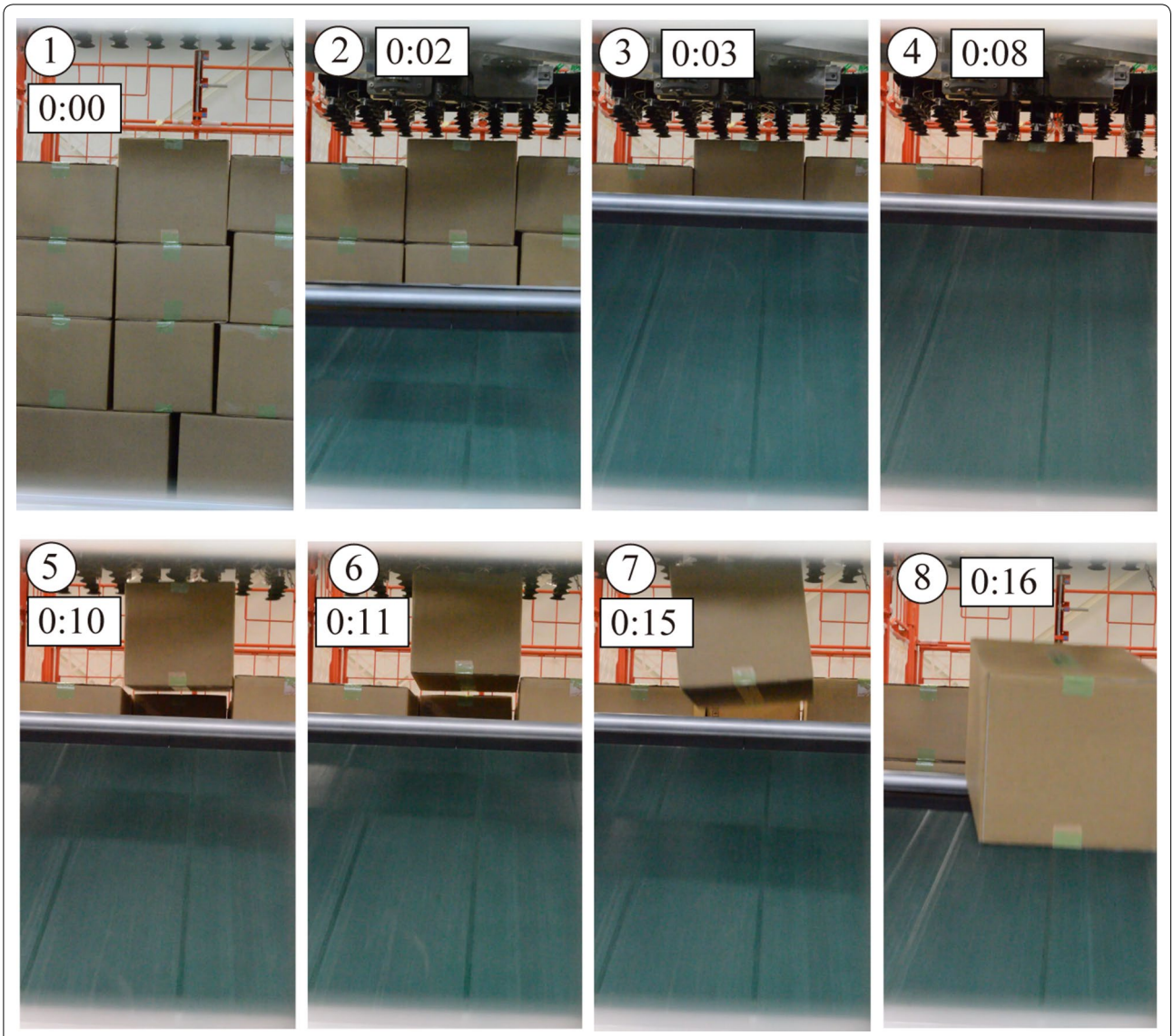


**Fig. 34** Part of the verification operation (extracting one cardboard box)

Similarly, Eq. (8) gives the relationship between the expansion and contraction amount $l_{ext2}$ (mm) of suction pad unit ② and the expansion time $t_{ext}$ (s).

$$l_{ext2} = 11.0t_{ext} \tag{8}$$

The difference in expansion and contraction amounts is likely influenced by the length of the high-strength wire material inside the bellows.

**Results of experiment 2-2: evaluation of allowable height difference between cardboard boxes by the end effector alone**

The experimental results confirmed that the developed end effector tolerates the target height difference of 80 mm or more between cardboard boxes, and results were acceptable up to 85 mm. We also confirmed that two boxes could be simultaneously held by allowing a height difference between boxes by a simple lowering motion of the main arm.

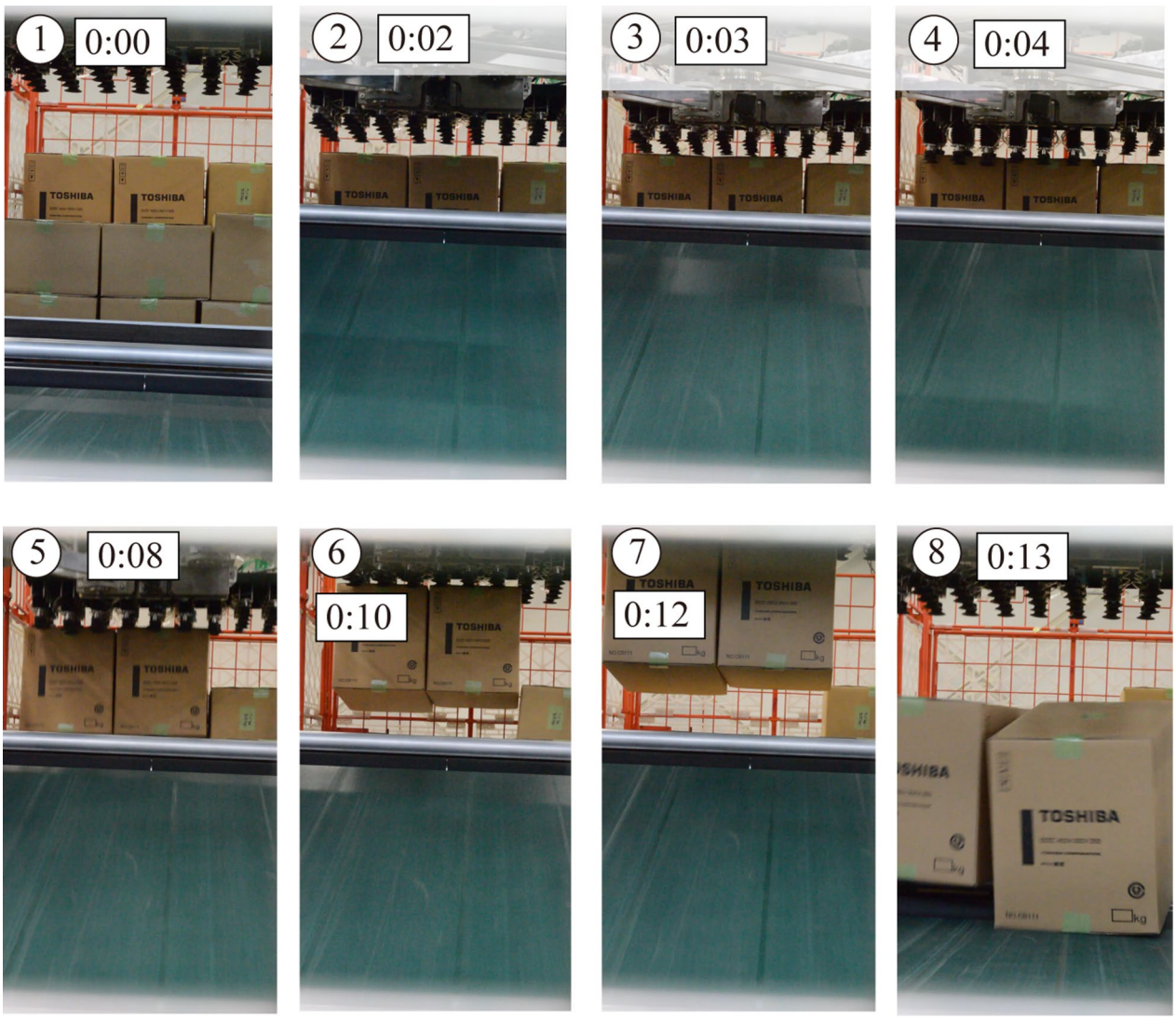


**Fig. 35** Part of the verification operation (extracting two cardboard boxes)

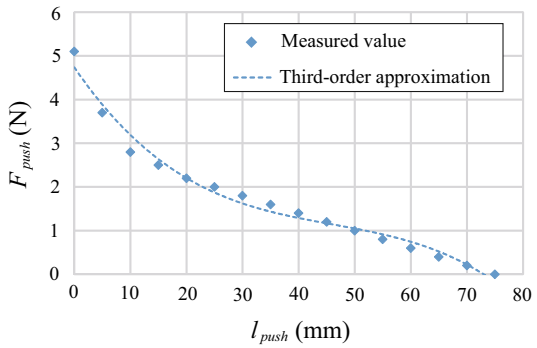


**Fig. 36** Relation between distance $l_{push}$ (mm) and maximum pressing force $F_{push}$ (N) of the developed suction pad unit

**Table 5 Experimental results for allowable inclination amount evaluations**

| $\theta_{inc}$ (°) | $l_{inc}$ (mm) | $l_{bent}$ (mm) |
|---|---|---|
| 10 | 63 | 25 |
| 20 | 52 | 40 |
| 30 | 45 | 45 |

### Results of experiment 2-3: evaluation of tilt tolerance of cardboard boxes by the end effector alone

The experimental results confirmed that a target inclination angle of up to 20° is acceptable. Even with a simple

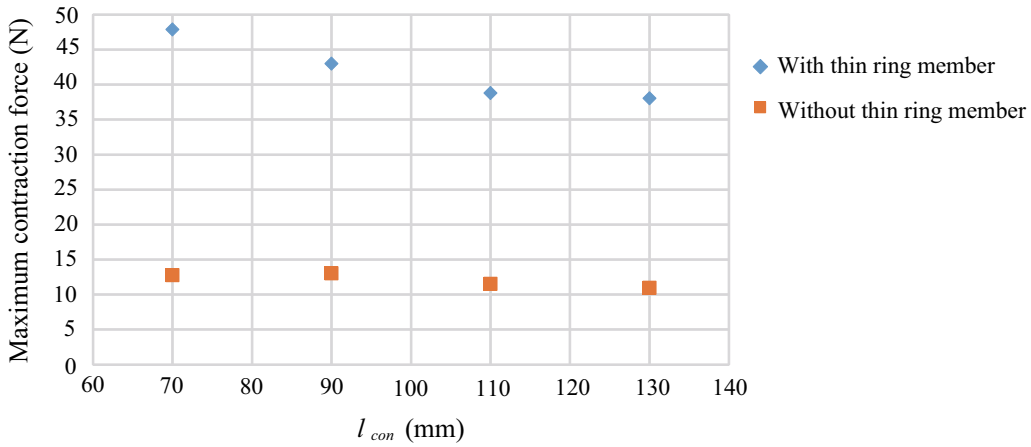


**Fig. 37** Relation between distance $l_{con}$ (mm) and maximum contraction force (N) of the developed suction pad unit

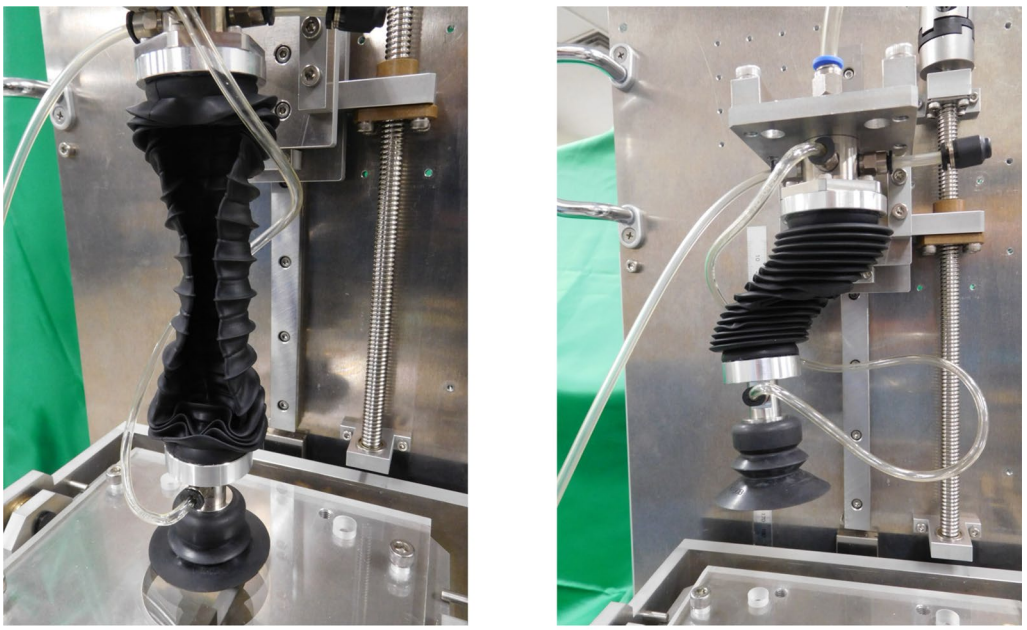


**Fig. 38** Experimental view of the contractile force evaluation. **a** Without thin ring members, **b** with thin ring members

lowering motion of the main arm, the suction pad surface followed the upper box surface by bending the bellows pneumatic actuator to hold the box. On the other hand, the number of suction pad units contacting the upper box surface decreased at inclinations exceeding 20°, so the box may shake and fall when lifted.

**Results of experiment 2-4: evaluation of contraction force by the end effector alone**

Figure 42 shows the state of the experiment, and Fig. 43 shows the results. The contraction force was 289 N when five suction pad units were used, 489 N with 10 units, 491 N with 15 units, 529 N with 20 units, 574 N with 25 units, and 701 N with 30 units. In Fig. 43, each experimental result is shifted on the time axis and superimposed. We confirmed that the contraction force increased with the number of suction pad units, despite

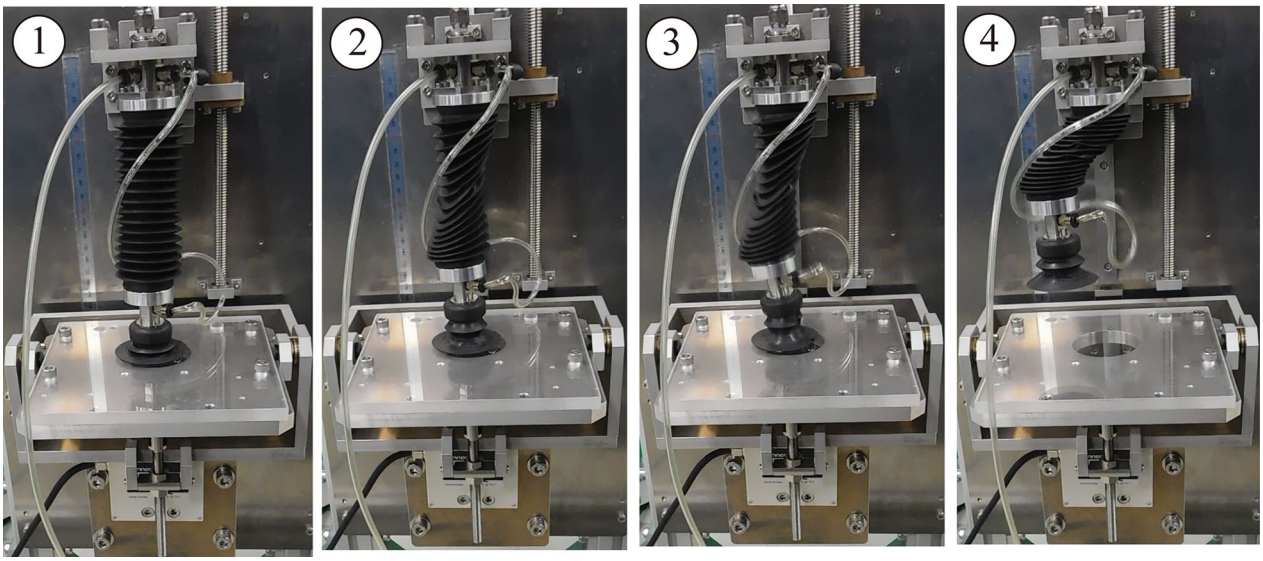


**Fig. 39** Deformation process of bellows pneumatic actuator

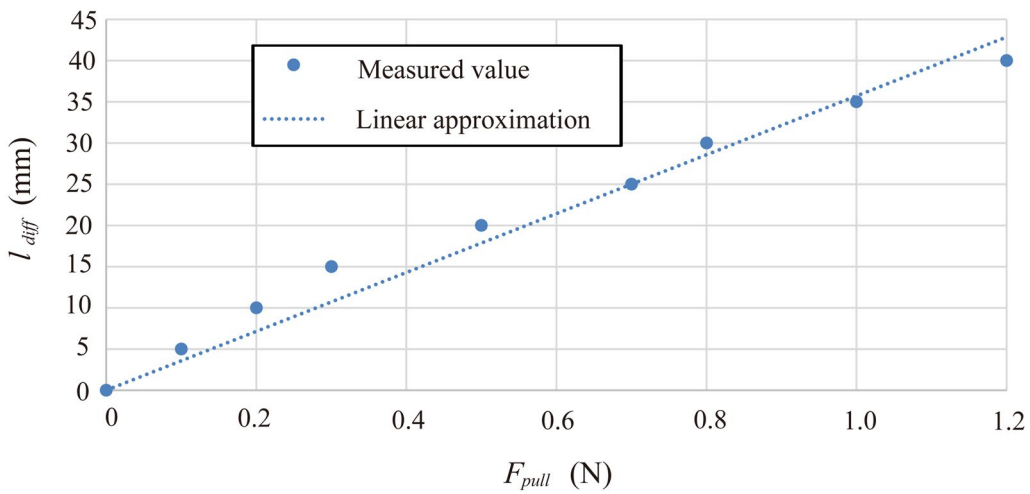


**Fig. 40** Experimental results of load and stretch length of bellows pneumatic actuator with ring member inside bellows

the curved deformation of the upper box surface. The suction pads separated from the upper surface of the box in each experiment, because the contraction force of the bellows pneumatic actuator exceeded the suction force of the suction pads. This experiment confirmed that it is possible to lift a cardboard box of 30 kg through contraction force of ten or more suction pad units.

#### Results of experiment 2-5: continuous transfer evaluation

The results confirmed that each box could be consecutively unloaded from a roll box pallet with no middle shelf by mutual action between the main arm and the conveyor arm of a linear motion-type depalletizing robot. The times required for each operation, shown in Tables 6, 7, 8 and 9, was obtained from log information. In Tables 6, 7, 8 and 9, the series operation times corresponding to Fig. 31 ②–⑥ is the time required for the main arm to start an operation from its initial posture, complete the operation, and return to the initial posture. The expansion time is the time from start to end of suction pad unit expansion in the reduced state. The expansion time occupancy rate is the ratio of expansion time to series operation time. The expansion time was about 5.4 s, and so took about 40%

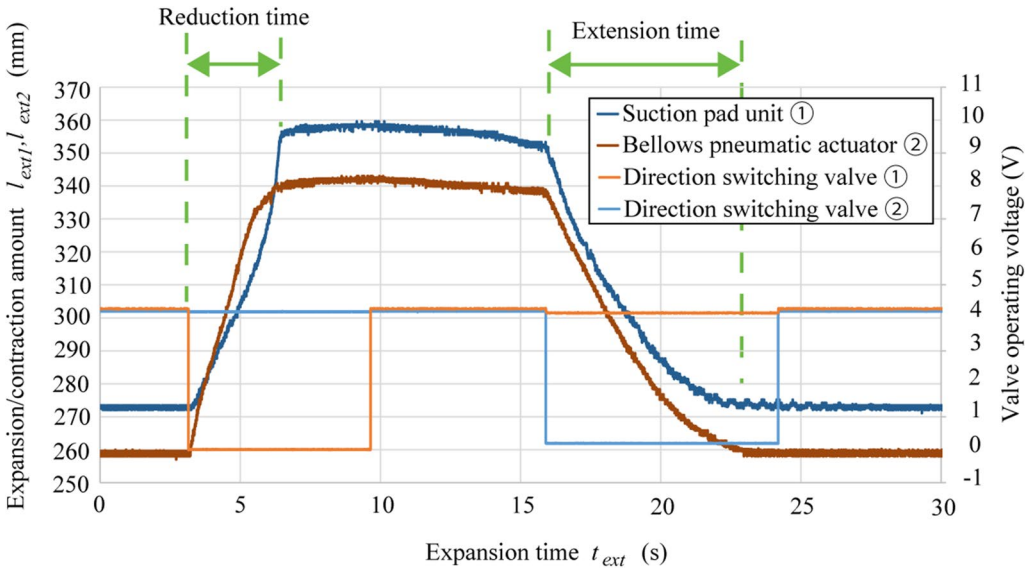


**Fig. 41** Experimental results from the expansion and contraction motion evaluation

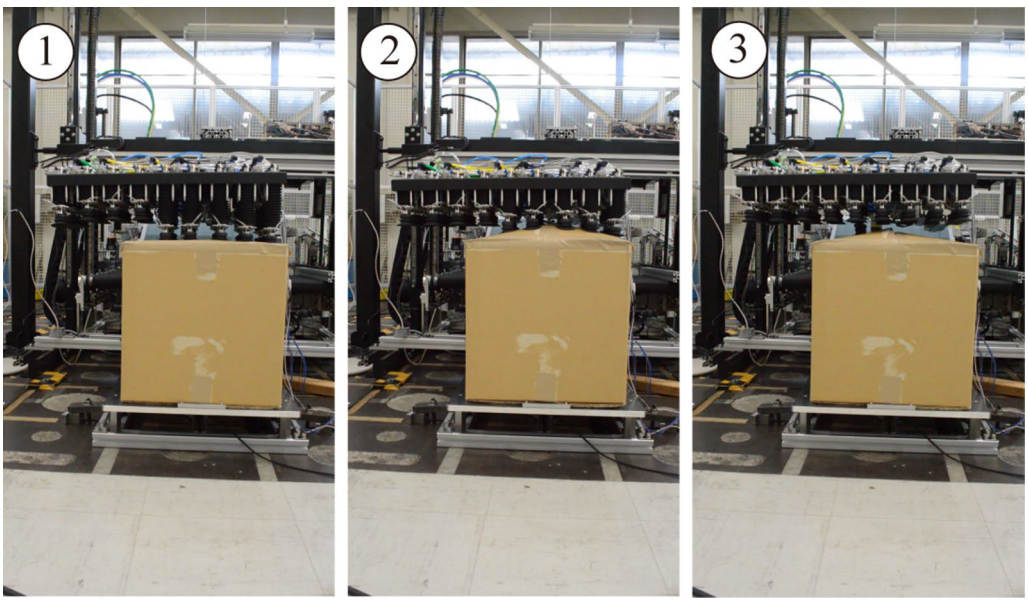


**Fig. 42** Experimental scene for evaluation of the contraction force of the end-effector alone

of the time in the series of transfer operations. Figure 44 shows the relation between elapsed times in each experiment and the remaining number of boxes in the roll box pallet. We found that if roll box pallet replacement time is not considered, the loading pattern for boxes in this section is equivalent to 320–350 packages per hour, exceeding the target of 300 packages or more per hour.

The bellows pneumatic actuator was not damaged during continuous unloading or other experiments. However, it might be damaged under long-term on-site use. In the future, it will be necessary to evaluate the actuator's durability in actual environments and to improve materials of the bellows pneumatic actuator.

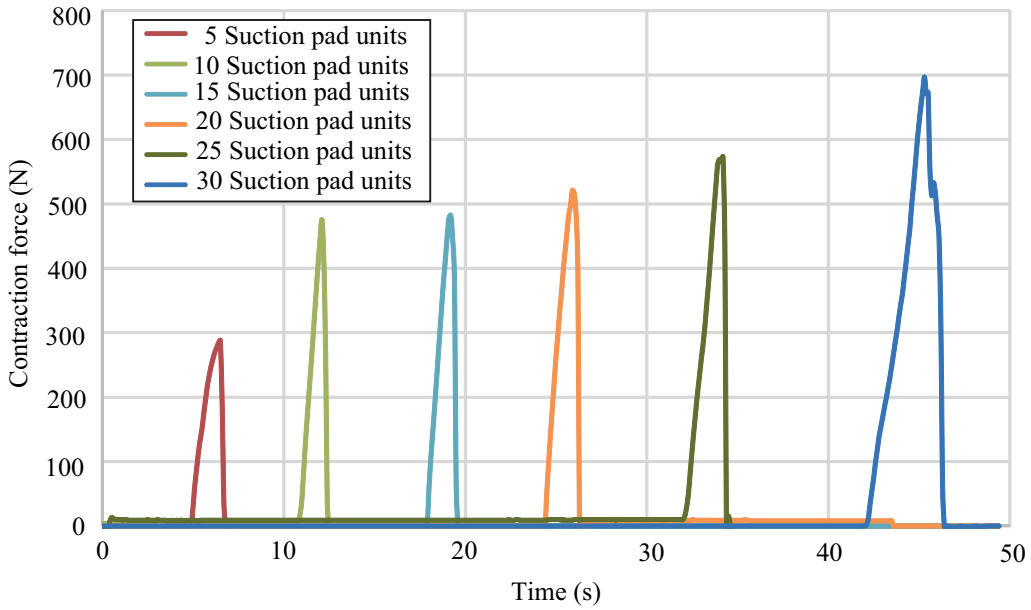


**Fig. 43** Experimental results for evaluation of contraction force by the end effector alone

**Table 6 Continuous unloading experiment results ①**

| No. | Notation | Difference in height (mm) | Series operation time (s) | Expansion operation | |
|---|---|---|---|---|---|
| | | | | Time (s) | Occupancy rate (%) |
| 1 | D-1 | – | 13.7 | 5.4 | 39.1 |
| 2 | C-4 | – | 12.3 | 5.4 | 43.6 |
| 3 | C-5 | – | 12.9 | 5.3 | 41.6 |
| 4 | B-5, C-6 | 20 | 14.2 | 5.4 | 38.1 |
| 5 | B-4 | – | 14.3 | 5.3 | 37.3 |
| 6 | B-3 | – | 16.2 | 5.4 | 33.5 |
| 7 | C-1, C-2 | 0 | 13.5 | 5.3 | 39.7 |
| 8 | C-3 | – | 15.2 | 5.4 | 35.5 |
| 9 | B-1, B-2 | 0 | 14.5 | 5.3 | 36.9 |
| 10 | A-3 | – | 13.1 | 5.3 | 40.1 |
| 11 | A-1, A-2 | 0 | 12.9 | 5.3 | 41.0 |
| 12 | A-4 | – | 14.8 | 5.2 | 35.4 |

**Table 7 Continuous unloading experiment results ②**

| No. | Notation | Difference in height (mm) | Series operation time (s) | Expansion operation | |
|---|---|---|---|---|---|
| | | | | Time (s) | Occupancy rate (%) |
| 1 | D-1 | – | 14.7 | 5.4 | 36.6 |
| 2 | C-5 | – | 12.8 | 5.3 | 41.8 |
| 3 | C-4 | – | 12.6 | 5.4 | 42.8 |
| 4 | B-5, C-6 | 20 | 14.3 | 5.3 | 37.4 |
| 5 | B-4 | – | 14.0 | 5.4 | 38.5 |
| 6 | B-3 | – | 13.8 | 5.3 | 38.7 |
| 7 | C-1, C-2 | 0 | 13.3 | 5.4 | 40.6 |
| 8 | C-3 | – | 14.6 | 5.4 | 37.1 |
| 9 | B-1, B-2 | 0 | 14.4 | 5.3 | 36.9 |
| 10 | A-2, A-3 | 0 | 13.4 | 5.4 | 40.1 |
| 11 | A-1 | – | 13.0 | 5.4 | 41.3 |
| 12 | A-4 | – | 14.3 | 5.4 | 37.6 |

## Discussion

We developed a new suction pad unit that applies a bellows pneumatic actuator to the support mechanism. As shown in Figs. 8, 9, the end effector using the suction pad unit proposed in this paper has two functions in contrast to end effectors using a conventional suction pad unit like the one shown in Fig. 5.

i. Reduction of contact pressing force.

ii. Realization of expansion and contraction with a thin structure.

We first describe quantitative effects regarding "(i) reduction of contact pressing force." The suction pad unit in conventional end effectors and the proposed end effector employ different methods for expansion and contraction. When the height difference between corrugated cardboard boxes is within the tolerable range of a conventional end effector, the commercially

**Table 8 Continuous unloading experiment results ③**

| No. | Notation | Difference in height (mm) | Series operation time (s) | Expansion operation | |
|---|---|---|---|---|---|
| | | | | Time (s) | Occupancy rate (%) |
| 1 | D-1 | – | 14.4 | 5.4 | 37.4 |
| 2 | C-5 | – | 12.9 | 5.3 | 41.0 |
| 3 | C-4 | – | 12.4 | 5.3 | 42.6 |
| 4 | B-5, C-6 | 20 | 13.6 | 5.2 | 38.5 |
| 5 | B-4 | – | 14.2 | 5.2 | 36.9 |
| 6 | C-1, B-3 | 45 | 13.2 | 5.2 | 39.5 |
| 7 | C-2 | – | 13.1 | 5.2 | 40.0 |
| 8 | C-3 | – | 14.6 | 5.2 | 35.8 |
| 9 | B-1, B-2 | 0 | 14.4 | 5.3 | 36.7 |
| 10 | A-1, A-2 | 0 | 13.0 | 5.3 | 40.5 |
| 11 | A-3 | – | 13.2 | 5.2 | 39.6 |
| 12 | A-4 | – | 14.8 | 5.3 | 35.6 |

**Table 9 Continuous unloading experiment results ④**

| No. | Notation | Difference in height (mm) | Series operation time (s) | Expansion operation | |
|---|---|---|---|---|---|
| | | | | Time (s) | Occupancy rate (%) |
| 1 | D-1 | – | 15.9 | 5.5 | 34.7 |
| 2 | C-5 | – | 12.3 | 5.3 | 42.9 |
| 3 | C-4 | – | 12.4 | 5.2 | 42.3 |
| 4 | B-5, B-4 | 0 | 14.6 | 5.3 | 36.3 |
| 5 | B-3, C-5 | 45 | 13.1 | 5.2 | 39.7 |
| 6 | C-6 | – | 13.9 | 5.2 | 37.5 |
| 7 | C-2 | – | 12.9 | 5.3 | 40.5 |
| 8 | C-3 | – | 14.8 | 5.3 | 35.4 |
| 9 | B-2 | – | 14.3 | 5.2 | 36.5 |
| 10 | B-1 | – | 14.2 | 5.3 | 36.9 |
| 11 | A-2, A-3 | 0 | 13.3 | 5.2 | 39.4 |
| 12 | A-1 | – | 12.4 | 5.2 | 42.2 |
| 13 | A-4 | – | 14.9 | 5.2 | 35.2 |

available suction pad unit shown in Fig. 5 is pressed against the upper surface of the cardboard box to reduce the height difference, so a large pressing force acts on the upper surface of the cardboard box. The maximum pressing force per conventional suction pad unit was about 7.7 N. In contrast, when the height difference between the cardboard boxes is within the tolerable range of the proposed end effector, the pressing force becomes smaller for the suction pad unit shown in Figs. 8, 9. The maximum pressing force by the proposed suction pad units was about 5.1 N per extension when the suction pad and the top surface of the cardboard box were in close contact. Furthermore, the greater the distance between the suction pad and the top surface of the cardboard box, the smaller the pressing force. As described above, since the suction pad unit of this paper has a small pressing force, it should be less likely to crush cardboard boxes.

We next describe the quantitative effects of "(ii) realization of expansion and contraction with a thin structure." In the proposed end effector, the amount of expansion and contraction is 85 mm for a height of 145 mm (Fig. 21). Dividing the amount of expansion and contraction by the height of the end effector gives 0.586 (=85/145). In contrast, the conventional end effector has an expansion–contraction amount of 50 mm for a height of 210 mm [4] (Fig. 7). Dividing the amount of expansion and contraction by the height of the end effector gives 0.238 (=50/210). This shows that the ratio of the amount of expansion and contraction with respect to the height of the end effector is improved in the proposed end effector. When inserting the end effector into the gap immediately below the middle shelf of a roll box pallet, the conventional end effector cannot enter a gap with a height 210 mm or less. On the other hand, the proposed end effector can enter a gap as small as 145 mm. Compared with the conventional suction pad unit (Fig. 5), the suction pad unit in which the bellows pneumatic actuator is applied to the support mechanism, the cardboard box can be prevented from being crushed, and a large amount of expansion and contraction and downsizing can be achieved. The end effector of depalletizing robot is composed of many suction pad units. Therefore, in the end effector of the depalletizing robot of this study, it is possible to reduce the thickness to enter a narrow gap, prevent breakage of the cardboard box, hold an inclined cardboard box, and simultaneously hold a plurality of cardboard boxes.

The results obtained in this study are summarized as follows.

- The suction pad unit alone had a mass of 267 g, an expansion and contraction amount of 85 mm, and a following angle of 30° (Figs. 8, 9 and 17). The suction pad unit in the stretched state realized suction holding of a 5.5 kg weight, contraction force of about 40–48 N (Figs. 19, 36).
- Single unit evaluations of the end effector revealed that the allowable height difference between boxes was 85 mm and the allowable inclination angle was 20° (Figs. 27, 28). Using 30 suction pad units, the bellows pneumatic actuator can realize a contraction force of 700 N or more (Fig. 43).
- A series of operations based on measured values from an RGB-D camera confirmed that the processing speed in continuous transfer operations was

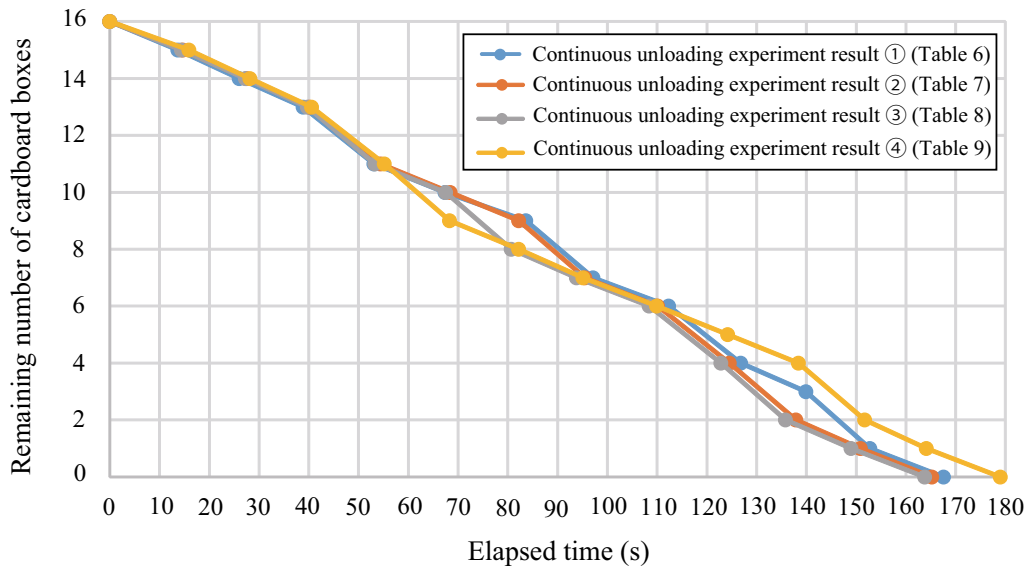


**Fig. 44** Relation between time and remaining number of boxes in each experiment

equivalent to 320–350 packages per hour under a prescribed loading pattern (Fig. 44).

The results of this study have practical significance because the activity area is expanded over that of a conventional depalletizing robot [4]. These results suggest that an end effector with multiple suction pad units, in which the bellows pneumatic actuator is applied to the support mechanism, has potentially good performance as a standard end effector for a depalletizing robot.

To further improve the quantitative effect of "(i) reducing the contact pressing force," it is possible to reduce the weight of the structural member of the suction pad and to reduce elasticity of the bellows by changing its materials. To further improve the quantitative effect of "(ii) realization of expansion and contraction with a thin structure," to realize structural thinning we could eliminate the tube joint and directly connect the tube and the structural member. One way to structurally realize large amount of expansion and contraction is to use a bellows material with improved elasticity, flexibility, and durability.

The present study was limited in that the expansion–contraction operation time of the bellows pneumatic actuator depends on the flow path. To speed up unloading operations in the future, it will be necessary to consider optimal flow path arrangements.

## Conclusion

This paper described the development of a thin vacuum suction-type end effector with the aim of expanding applications for linear motion-type depalletizing robots that can simultaneously extract multiple cardboard boxes. The end effector in this paper is equipped with up to 50 suction pad units that apply a bellows pneumatic actuator to the support mechanism. The proposed device improves load resistance due to a high-strength wire placed inside the bellows, and improves contraction force due to ring members placed inside the ridges of the bellows. We fabricated the proposed end effector and attached it to a conventional linear motion-type depalletizing robot for verification experiments. Height differences between boxes and box inclinations were tolerated by simple vertical movement of the main arm, thus achieving box extraction. We confirmed the usefulness of the developed end effector through a series of unloading operations.

In future studies, we will study methods for sensing the state of cardboard boxes directly beneath a shelf to realize continuous unloading operations from roll box pallets with a middle shelf.

**Acknowledgements**
Not applicable.

**Authors' contributions**
JT contributed to the development of the proposed suction pad units and was the lead experimenter. AO, HN, TS, and HE contributed to the development of the linear motion-type depalletizing robot and supported the

experiment. JT drafted the manuscript, and AO, HN, TS, and HE revised and refined the manuscript. All authors read and approved the final manuscript.

**Funding**
Not applicable.

**Availability of data and materials**
Not applicable.

**Competing interests**
The authors declare that they have no competing interests.

Received: 18 July 2019 Accepted: 26 December 2019
Published online: 03 January 2020

**References**

1. Echelmeyer W, Kirchheim A, Wellbrock E (2008) Robotics-logistics: challenges for automation of logistic processes. In: Proceedings of IEEE international conference on automation and logistics, pp 2099–2103. https://doi.org/10.1109/ICAL.2008.4636510
2. Katsoulas D, Bergen L, Tassakos L (2002) A versatile depalletizer of boxes based on range imagery. In: Proceedings of IEEE international conference on robotics and automation (ICRA), pp 4313–4319. https://doi.org/10.1109/ROBOT.2002.1014438
3. Katsoulas DK, Kosmopoulos DI (2001) An efficient depalletizing system based on 2D range imagery. In: Proceedings of IEEE international conference on robotics and automation (ICRA), pp 305–312. https://doi.org/10.1109/ROBOT.2001.932570
4. Nakamoto H, Eto H, Sonoura T, Tanaka J, Ogawa A (2016) High-speed and compact depalletizing robot capable of handling packages stacked complicatedly. In: Proceedings of IEEE/RSJ international conference on intelligent robots and systems (IROS), pp 344–349. https://doi.org/10.1109/IROS.2016.7759077
5. Hasegawa S, Wada K, Okada K, Inaba M (2019) A three-fingered hand with a suction gripping system for warehouse automation. J Robot Mechatron 31(2):289–304. https://doi.org/10.20965/jrm.2019.p0289
6. Komoda K, Sugahara A, Nakamoto H, Ogawa A, Hatanaka Y (2019) Mobile picking-Robot having wide reach area for shelves. In: 2019 IEEE/SICE international symposium on system integration (SII), pp 210–215. https://doi.org/10.1109/SII.2019.8700409
7. Nakamoto H, Ohtake M, Komoda K, Sugahara A, Ogawa A (2018) A gripper system for robustly picking various objects placed densely by suction and pinching. In: Proceedings of IEEE/RSJ international conference on intelligent robots and systems (IROS), pp 6093–6098. https://doi.org/10.1109/IROS.2018.8593887
8. Zhu H, Kok YY, Causo A, Chee KJ, Zou Y, Al-Jufry SOK, Liang C, Chen IM, Cheah CC, Low KH (2016) Strategy-based robotic item picking from shelves. In: Proceedings of IEEE/RSJ international conference on intelligent robots and systems (IROS), pp 2263–2270. https://doi.org/10.1109/iros.2016.7759354
9. Schwarz M, Milan A, Periyasamy AS, Behnke S (2018) RGB-D object detection and semantic segmentation for autonomous manipulation in clutter. Int J Robot Res 37(4–5):437–451. https://doi.org/10.1177/0278364917713117
10. Schulte HF (1961) The characteristics of the McKibben artificial muscle. The application of external power in prosthetics and orthotics, pp 94–115
11. Niiyama R, Nishikawa S, Kuniyoshi Y (2012) Biomechanical approach to open-loop bipedal running with a musculoskeletal athlete Robot. Adv Robot 26(3–4):383–398. https://doi.org/10.1163/156855311X614635
12. Hitzmann A, Masuda H, Ikemoto S, Hosoda K (2018) Anthropomorphic musculoskeletal 10 degrees-of-freedom robot arm driven by pneumatic artificial muscles. Adv Robot 32(15):865–878. https://doi.org/10.1080/01691864.2018.1494040
13. Kurumaya S, Suzumori K, Nabae H, Wakimoto S (2016) Musculoskeletal lower-limb robot driven by multifilament muscles. Robomech J 3:18. https://doi.org/10.1186/s40648-016-0061-3
14. Dameitry A, Tsukagoshi H (2017) Lightweight pneumatic semiuniversal hand with two fingers aimed for a wide range of grasping. Adv Robot 31(23–24):1253–1266. https://doi.org/10.1080/01691864.2017.1392346
15. Tsukagoshi H, Kitagawa A, Kamata Y (2002) Wearable fluid power composed of transformed flat tube actuators. In: Proceedings of IEEE/RSJ international conference on intelligent robots and systems (IROS), pp 1178–1183. https://doi.org/10.1109/IRDS.2002.1043892
16. Tsukagoshi H, Mori Y, Kitagawa A (2012) Fast accessible rescue device by using a flexible sliding actuator. In: Proceedings of IEEE international conference on robotics and automation (ICRA), pp 1175–1180. https://doi.org/10.1109/icra.2012.6224982
17. Wakimoto S, Suzumori K, Ogura K (2011) Miniature pneumatic curling rubber actuator generating bidirectional motion with one air-supply tube. Adv Robot 25(9–10):1311–1330. https://doi.org/10.1163/016918611X574731
18. Marchese AD, Rus D (2016) Design, kinematics, and control of a soft spatial fluidic elastomer manipulator. Int J Robot Res 35(7):840–869. https://doi.org/10.1177/0278364915587925
19. Marchese AD, Onal CD, Rus D (2014) Autonomous soft robotic fish capable of escape maneuvers using fluidic elastomer actuators. Soft Robot l(1):75–87. https://doi.org/10.1089/soro.2013.0009
20. Katzschmann RK, Marchese AD, Rus D (2015) Autonomous object manipulation using a soft planar grasping manipulator. Soft Robot 2(4):155–164. https://doi.org/10.1089/soro.2015.0013
21. Felt W, Robertson MA, Paik J (2018) Modeling vacuum bellows soft pneumatic actuators with optimal mechanical performance. In: Proceedings of IEEE international conference on soft robotics (RoboSoft), pp 534–540. https://doi.org/10.1109/ROBOSOFT.2018.8405381
22. Usevitch NS, Okamura AM, Hawkes EW (2018) APAM: antagonistic pneumatic artificial muscle. In: Proceedings of IEEE international conference on robotics and automation (ICRA), pp 1539–1546. https://doi.org/10.1109/ICRA.2018.8460881
23. Belforte G, Eula G, Ivanov A, Visan AL (2014) Bellows textile muscle. J Text Inst 105(3):356–364. https://doi.org/10.1080/00405000.2013.840414
24. Lee J, Rodrigue H (2019) Origami-based vacuum pneumatic artificial muscle with large contraction ratio. Soft Robot 6(1):109–117. https://doi.org/10.1089/soro.2018.0063

## Publisher's Note